THE ROLE OF YJEQ GTPASE IN BACTERIAL RIBOSOME BIOGENESIS

THE ROLE OF THE YJEQ GTPASE IN BACTERIAL RIBOSOME BIOGENESIS: FUNCTION OF THE C-TERMINAL ZINC-FINGER DOMAIN

By: **AJITHA JEGANATHAN, B.SC**

A Thesis Submitted to the School of Graduate Studies in Partial Fulfillment of the Requirements for the Degree Master of Science

McMaster University

McMaster University MASTER OF SCIENCE (2014)

Hamilton, Ontario (Biochemistry and Biomedical Sciences)

TITLE:	The Role of the YjeQ GTPase in Bacterial Ribosome Biogenesis: Function of the C-terminal Zinc-finger Domain
AUTHOR:	Ajitha Jeganathan, B.Sc (University of Toronto)
SUPERVISOR:	Dr. Joaquin Ortega
NUMBER OF PAGES:	viii, 79

ABSTRACT

Our understanding of the mechanism of ribosome assembly in bacteria is still in its infancy. Work from our laboratory and others have recently established that some protein assembly factors assist the assembly process at its late stages, mediating the correct folding of the functional core of the 30S and 50S subunits. The GTPase YjeQ is an assembly factor that displaces the upper domain of h44 of the mature 30S subunit upon binding, inducing a distortion in the decoding center. We hypothesized that the displacement of h44 is caused by the zinc-finger domain of YjeQ and mediates the release of RbfA, another assembly factor involved in 30S subunit maturation. To understand how the zinc-finger domain of YjeQ implements the functional interplay with RbfA, we constructed several deletion mutants of the domain. We found that the zinc-finger domain of YjeQ was required to bind the 30S subunit, but not the C-terminal extension (CTE) of the domain. The CTE was necessary for stimulation of GTPase activity upon binding to the 30S subunit and removal of bound RbfA from the 30S subunit. The data presented here suggests that the zinc-finger domain is essential for YjeQ to bind the 30S subunit and to implement the functional interplay with RbfA. Ongoing structural studies of the complex formed by the YjeQ CTE variant and the 30S subunit will provide a three dimensional view of the conformational changes that occur to implement the functional interplay between YjeQ and RbfA at the late stages of 30S subunit assembly.

ACKNOWLEDGEMENTS

First I would like to express my sincerest gratitude to my supervisor, Dr. Joaquin Ortega, for his support and guidance during the course of my graduate studies. You have allowed me to continue my passion for science and instilled values in me that I will carry into my future career and life choices. I would also like to thank my committee members, Dr. Eric Brown and Dr. Michael Surette, for their valuable insight and advice in the progression of this project.

I would like to thank all members of the Ortega lab, past and present, for helpful discussions and technical support. I would like to extend a special thanks to Vivian Leong for bearing with me through many technical hurdles and always having an answer to my infinite questions. I would also like to thank Dr. Alba Guarné and her lab for sharing their equipment and knowledge with me.

I would like to thank Matthew Sapiano for technical support with the Circular Dichroism experiments and Jonathan Stokes for assistance with attaining the *in vivo* growth curves and discussion on ribosome assembly.

I would like to extend a very special thanks to my family and friends who have played a key role in providing me with moral support during my graduate studies. In particular, I would like thank my parents and siblings, who constantly provide me with unconditional love and support. You have all been my motivation and strength on a daily basis. Finally, to my boyfriend Arun Manoharan, thank you for being my rock. You were the voice I needed to hear on good days and bad ones. You kept me going and really are my other half.

TABLE OF CONTENTS

ABSTRACT	iii
ACKNOWLEDGEMENTS	iv
TABLE OF CONTENTS	v
LIST OF FIGURES AND TABLES	vi
LIST OF ABBREVIATIONS AND SYMBOLS	vii
1. INTRODUCTION	1
1.1 The bacterial ribosome	1
1.2 Bacterial ribosome biogenesis	2
1.3 Ribosome assembly factors	5
1.4 YjeQ (RsgA – Ribosomal Small Subunit GTPase)	7
1.5 YjeQ and assembly of the 30S subunit	11
1.6 Interplay of YjeQ and RbfA	16
2. **MATERIALS AND METHODS**	20
2.1 Cell lines and protein constructs	20
2.2 Purification of YjeQ and YjeQ variants	21
2.3 Purification of RbfA	23
2.4 Purification of ribosome particles	24
2.5 Circular dichroism for YjeQ folding analysis	26
2.6 Binding assays	27
2.7 GTPase activity assays	29
2.8 *In vivo* complementation assays	30
3. RESULTS	33
3.1 Characterization of YjeQ C-terminal truncation variants	33
3.2 YjeQ requires the zinc-finger domain to bind the 30S particle	37
3.3 The CTE of YjeQ is necessary for 30S subunit-dependent GTPase activity	42
3.4 YjeQ in unable to remove RbfA from the 30S subunit without the CTE	45
3.5 The M3 variant is unable to complement the function of YjeQ *in Vivo*	50
3.6 The zinc-finger domain of YjeQ is unlikely to interact with the head of the 30S subunit	55
4. DISCUSSION	59
4.1 The role of the zinc-finger domain of YjeQ in 30S subunit Biogenesis	60
4.2 The zinc-finger domain of YjeQ plays a critical role to its function *in vivo*	63
4.3 Mechanism of YjeQ and RbfA interaction on the 30S subunit	65
5. REFERENCES	69

LIST OF FIGURES AND TABLES

Figure 1	Structure of the *E. coli* 30S subunit	2
Figure 2	Structure of the YjeQ protein	7
Figure 3	The immature 30S subunit from Δ*yjeq E. coli*	12
Figure 4	Complex of *E. coli* YjeQ with 30S subunit	15
Figure 5	Structure of the complex of RbfA with the 30S subunit	17
Figure 6	YjeQ C-terminal variants	34
Figure 7	Circular dichroism spectra of YjeQ C-terminal variants	36
Figure 8	Purification and characterization of the mature and immature 30S particles	38
Figure 9	Binding of YjeQ C-terminal variants to the 30S particles	41
Figure 10	Pelleting Assay of M3 variant with the mature 30S subunit	42
Figure 11	GTPase activity of YjeQ C-terminal variants	44
Figure 12	Interplay of YjeQ and RbfA on the 30S particle	47
Figure 13	Interplay of the M3 variant of YjeQ with RbfA on the mature 30S subunit	49
Figure 14	Growth and rRNA analysis of *E. coli* strains	51
Figure 15	Ribosome profiles of *E. coli* strains	54
Figure 16	Orientation of YjeQ bound to the 30S subunit solved by Gao lab	57
Figure 17	Model of YjeQ and RbfA interplay with the 30S particle	68

Table 1	YjeQ C-terminal variant mutagenesis primers	20
Table 2	Doubling-time and growth rates of the *E. coli* strains in LB liquid media	50

LIST OF ABBREVIATIONS AND SYMBOLS

Θ	Molar ellipticity
A_{260}	Light absorbance at 260 nanometres (wavelength)
BSA	Bovine serum albumin
Cryo-EM	Cryo-electron microscopy
C-Terminal	Carboxyl-terminus
CTE	C-terminal extension (C-terminal helix of zinc-finger domain of YjeQ)
Δ*abcD*	Delta, signifying deletion of gene *abcD*
DNA	Deoxyribonucleic acid
DNAse	Deoxyribonuclease
DTT	Dithiothreitol
E. coli	*Escherichia coli*
EDTA	Ethylenediaminetetraacetic acid
EMDB	Electron Microscopy Data Bank
Era	*E. coli* ras-like protein
FPLC	Fast protein liquid chromatography
GDP	Guanosine diphosphate
GTP	Guanosine-5'-triphosphate
GTPase	Guanosine triphosphate hydrolase
GMP-PNP	5'-Guanylyl imidodiphosphate – non-hydrolyzable analog of GTP
GDPNP	Guanosine 5’-(tetrahydrogen triphosphate) – non-hydrolyzable analog of GTP
h44	Helix 44 of the 16S rRNA of the 30S subunit
h45	Helix 45 of the 16S rRNA of the 30S subunit
IF2	Initiation factor 2
IF3	Initiation factor 3
IPTG	Isopropyl β-D-1-thiogalactopyranoside
iTRAQ	Isobaric tags for relative and absolute quantitation
K_{CAT}	constant that describes the turnover rate of an enzyme-substrate complex to product and enzyme
K_M	Michaelis constant that describes the amount of substrate needed for the enzyme to obtain half of its maximum rate of reaction
KsgA	Kasugamycin resistance protein
LB	Luria-Bertani broth

Mg^{2+}	Magnesium ion
MOPS	3-(N-morpholino)propanesulfonic acid
mRNA	Messenger RNA
Ni^{2+}	Nickel ion
N-terminal	Amino-terminal
OB-fold	Oligosaccharide-binding fold
OD_{600}	Optical Density of light at wavelength 600 nanometres
PDB	Protein Data Bank
PBS	Phosphate buffered saline
RbfA	Ribosome binding factor A
RbgA	Ribosome biogenesis GTPase A
RID	Ribosome interaction domain
RimM	Ribosome maturation factor M
RNA	Ribonucleic acid
RNase	Ribonuclease
r-protein	Ribosomal protein
rRNA	Ribosomal RNA
RsgA	Ribosome stimulated GTPase A (YjeQ)
S1-S21	Small ribosomal proteins 1 to 21
SDS-PAGE	Sodium dodecyl sulfate-Polyacrylamide gel electrophoresis
S. typhimurium	Salmonella *typhimurium*
tRNA	Transfer RNA
WT	Wild type (parental)
Zn^{2+}	Zinc ion

1. Introduction

1.1 The bacterial ribosome

The ribosome is a ribonucleoprotein complex that is responsible for the translation of proteins in prokaryotic and eukaryotic cells. The bacterial ribosome sediments as a 70S subunit during ultracentrifugation (Tissieres and Watson, 1958) and is composed of two functional subunits. The first is the large 50S subunit, composed of 23S and 5S rRNA as well as 34 ribosomal proteins (Kaltschmidt and Wittmann, 1970;Shajani *et al*., 2011). The 50S subunit houses the peptidyl transferase centre, which is responsible for peptide bond formation of incoming aminoacyl-tRNAs. The second is the small 30S particle, composed of 16S rRNA and 21 ribosomal proteins. The 16S rRNA folds into a four-domain structure with the help of ribosomal proteins, which correspond to key landmarks of the 30S subunit: the body (5' domain), the platform (central domain), the head (3' major domain) and helix 44 (3' minor domain) (Figure 1) (Wimberly *et al*., 2000). The 30S subunit is home to the decoding centre which is involved in correct base pairing of the mRNA codon and tRNA anti-codon to ensure translational fidelity of the ribosome. Adenine residues (A1492 and A1493) that monitor this process are found on helix 44 (h44) (Lescoute and Westhof, 2006). With the help of translation factors and tRNA, these two subunits are able to coordinate the precise and efficient translation of mRNA into peptides.

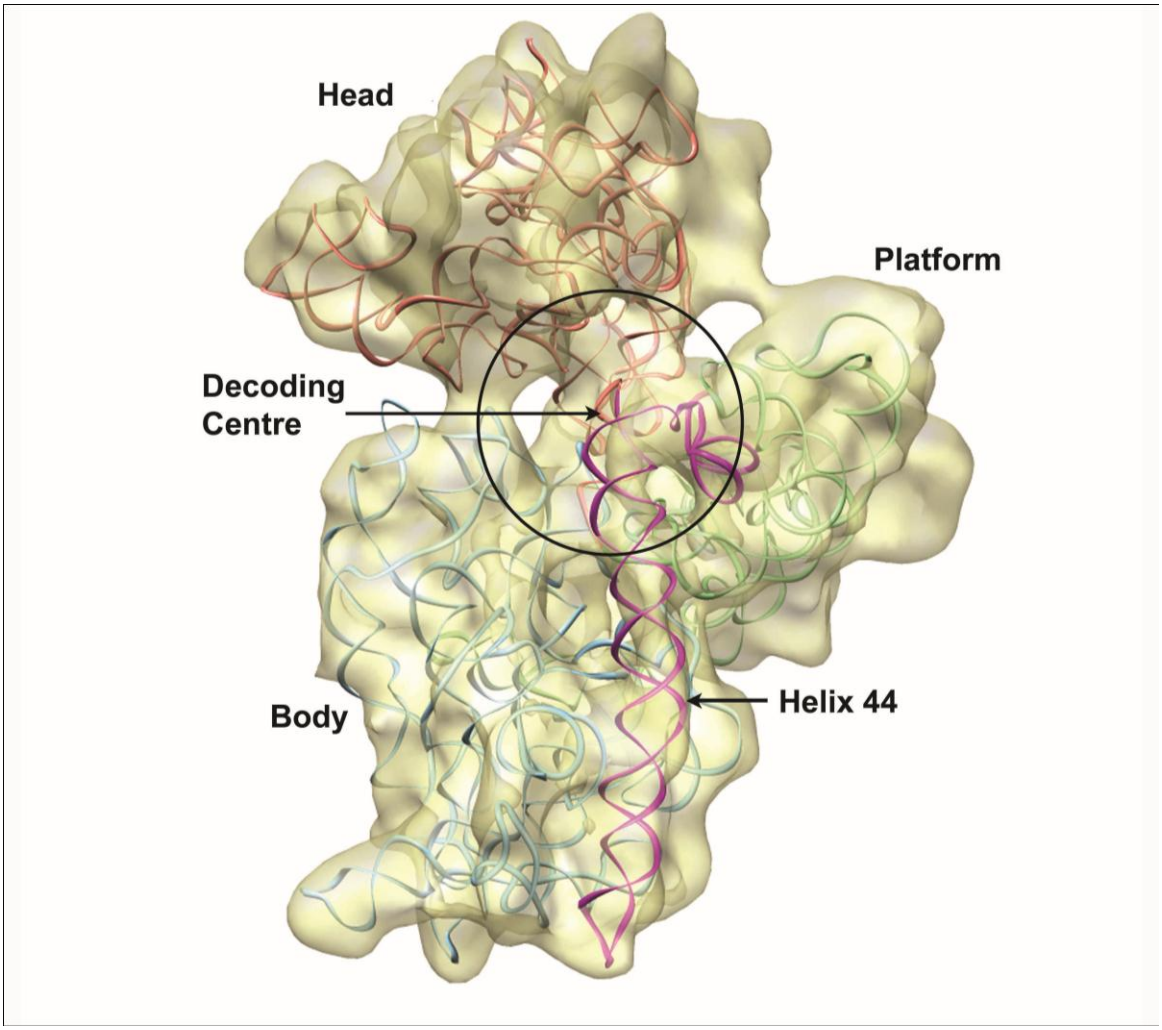

Figure 1. Structure of the *E. coli* 30S subunit. The 30S subunit of the bacterial ribosome is viewed from the interface side that interacts with the 50S subunit. The structure consists largely of the 16S rRNA that is characterized by four key folding domains that form the landmarks of the 30S subunit: Body (5' domain, blue), Platform (central domain, green), Head (3' major domain, pink) and Helix 44 (3' minor domain, magenta). The 21 ribosomal proteins that bind the 16S rRNA are not shown in the docked crystal structure of the 30S subunit, but are represented by the remaining cryo-EM density. (EMDB 1775 fitted with PDB 2AVY).

1.2 Bacterial ribosome biogenesis

The ribosome must perform the function of protein translation with accuracy and efficiency, since the products of this process are required for the

viability, structural integrity and house-keeping of all living cells. For this reason it must also be assembled with precision, speed and in a regulated manner. Considering the size and complexity of this macromolecule, it has been difficult to understand its assembly process.

Pioneering studies of ribosomal assembly were conducted *in vitro* and demonstrated that both subunits could individually be assembled into functioning ribosomes by combining their components, ribosomal proteins and rRNA (Nierhaus and Dohme, 1974; Traub and Nomura, 1968). Through *in vitro* studies, these groups were able to create a hierarchal map of binding of ribosomal proteins to rRNA by changing the order in which the proteins were added to rRNA in solution (Held *et al*., 1974; Mizushima and Nomura,1970; Rohl and Nierhaus, 1982; Spillmann et al., 1977). The assembly of ribosomes *in vitro* demonstrated that some of the protein binding events were thermodynamically interdependent and reconstitution intermediates were generated upon changes in temperature or ionic strength of the reaction. The assembly maps paved the path for research on ribosomal assembly and to date have remained nearly intact (Chen and Williamson, 2013). However, the conditions to reconstitute the ribosome *in vitro* are very different to the physiological conditions in the cell. The *in vitro* reconstitutions required low and high ionic strength, temperature and pH, as well as several hours to result in a functioning ribosome. This suggests that there are factors within the cell that may help the ribosome to overcome kinetic traps during assembly.

In the last decade, the *in vivo* assembly studies of bacterial ribosomes have uncovered information about ribosome biogenesis that *in vitro* studies were not able to uncover. In the cell, the ribosome only takes a few minutes to assemble and proceeds while the rRNA is being transcribed in the 5'-3' direction (de Narvaez and Schaup, 1979; Lindahl, *et al.*, 1975). Initially, the bacterial cell produces all three rRNA transcripts (23S, 16S and 5S) on a primary transcript (Shajani *et al*., 2011). These are cleaved by RNAse III into the precursor rRNA (precursor 23S rRNA, 17S rRNA and 9S rRNA respectively) (Ginsburg and Steitz, 1975). The 17S rRNA of the 30S ribosome undergoes the most processing and 115 nucleotides are cleaved at the 5' end by RNAse E and RNAse G (Li *et al*., 1999). The 3' end involves cleavage of 33 nucleotides and it has been linked to exoribonucleases: RNases II, R, PH and polynucleotide phosphorylase (PNPase) (Sulthana and Deutscher, 2013) as well as YbeY (Davies *et al*., 2010; Jacob *et al*., 2013).

As mentioned earlier, the order of binding of ribosomal proteins to all three rRNA has not changed significantly since the Nomura and Nierhaus maps were derived (Nierhaus and Dohme, 1974; Traub and Nomura, 1968). More recently, the hierarchy of ribosomal protein binding, rRNA folding structure and rate have been verified and modified through the use of novel stable isotope pulse-chase (Bunner *et al*., 2008; Talkington *et al*., 2005), hydroxyl radical foot-printing (Adilakshmi *et al*., 2008) and cryo-electron microscopy (Mulder *et al*., 2010). The hierarchal map of ribosomal proteins reveals that while some ribosomal proteins

are able to stably bind rRNA (1˚-primary binding protein), others depend on previously bound 1˚ binders (2˚-secondary binding protein) or 2˚ binders to bind (3˚-tertiary binding protein). This reveals that ribosomal assembly proceeds in a precise manner that is very much dependent on specific protein-rRNA interactions. More recently, an *in vivo* study using multi-prone quantitative mass spectroscopy was able to recreate a modern Nomura and Nierhaus map of binding for both the 30S and 50S subunits within the bacterial cell (Chen and Williamson, 2013).

1.3 Ribosome assembly factors

Ribosome reconstitution experiments have demonstrated that ribosomes assemble quickly and efficiently *in vivo* without requiring harsh changes in temperature, pH or ionic conditions. These conditions are likely required *in vitro* in order to help rRNA overcome kinetic traps that occur when folding with ribosomal proteins (Shajani *et al*., 2011). However, *in vivo* there are ribosome assembly factors that may act as chaperones to limit the amount of non-functional ribosome intermediates formed. Their functions may entail facilitating proper rRNA folding and protein-RNA interactions during assembly. These factors include rRNA and protein modification enzymes, endonucleases, RNAses, helicases, GTPases and proteins whose exact function is still to be determined (Connolly and Culver, 2013). To date there have been more than 20 assembly factors that have been identified whose absence results in a slow-growth phenotype of cells and defective ribosome profiles (Shajani *et al*., 2011).

These assembly factors are not part of the final structure of the ribosome and tend to be generally conserved across Gram-positive and Gram-negative bacteria (Wilson and Nierhaus, 2007). Most ribosomal assembly factors are not essential to cell growth, unless they play dual roles in other cellular processes. However, in the case of eukaryotic cells over a hundred assembly factors have been identified, many of which are essential for cell survival (Strunk and Karbstein, 2009). This is likely due to the fact that the eukaryotic ribosome is much larger and more complex. It also requires additional proteins to shuttle the ribosome between the cytoplasm and nucleolus during assembly.

Among the bacterial assembly factors are a set of factors that appear to contribute in a related manner to the assembly of the small 30S subunit. These assembly factors are YjeQ (RsgA), RbfA, Era and RimM. These factors are of particular interest because some or all of them have been connected to each other through genetic (Bylund *et al*., 1998; Campbell and Brown, 2008; Inoue *et al*., 2003; Inoue *et al*., 2006), biochemical (Goto *et al*., 2011) and structural studies (Clatterbuck Soper *et al*., 2013; Datta *et al*., 2007; Guo *et al*., 2011; Guo *et al*., 2013; Jomaa *et al*., 2011a; Jomaa *et al*., 2011b; Leong *et al*., 2013; Sharma *et al*., 2005). These factors act in the late stages of assembly of the 30S subunit. Removal or depletion of these factors cause the cells to accumulate immature 30S subunits that contain unprocessed 17S rRNA (Bylund *et al*., 1998; Himeno *et al*., 2004; Jomaa *et al*., 2011a; Sayed *et al*., 1999; Xia *et al*., 2003).

This thesis will particularly focus on the function of YjeQ and its functional interplay with RbfA.

1.4 YjeQ (RsgA – Ribosomal Small Subunit GTPase)

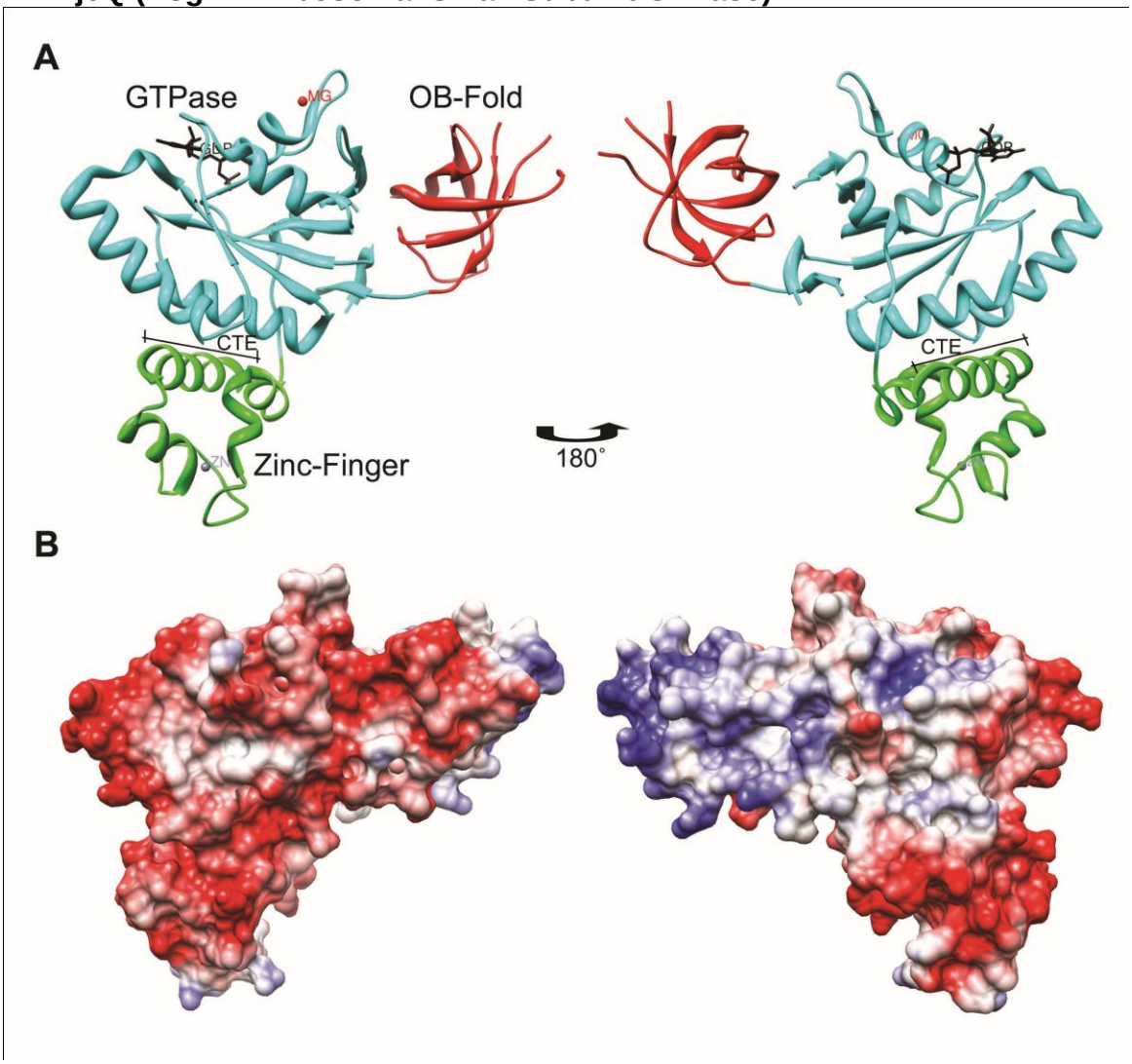

Figure 2. Structure of the YjeQ protein. (A) The *S. typhimurium* YjeQ protein is represented by the three domains: The N-termnial OB-fold domain (red), central GTPase domain (blue) and the c-terminal zinc-finger domain (green). The C-terminal extension (CTE) of the zinc-finger domain is the C-terminal helix. The GTPase domain coordinates Mg^{2+} (red) and binds nucleotides, in this case GDP (black). The zinc-finger domain coordinates Zn^{2+} (grey). (B) The electrostatic surface potential of YjeQ. Zones are negatively charged (red), positively charged (blue) and uncharged (white). (Left panel) Solvent exposed surface; (right panel) 30S interface surface. (PDB 2RCN)

YjeQ was originally identified as an essential gene for bacterial growth in culture (Arigoni *et al*., 1998) that had a slow steady-state GTPase activity (Daigle *et al*., 2002). Studies of *yjeQ* deletion mutants found that the gene was non-essential but caused a slow-growth phenotype of cells and an accumulation of free 30S subunits containing unprocessed 17S rRNA (Himeno *et al*., 2004; Jomaa *et al*., 2011a). YjeQ was able to bind the 30S subunit and its GTPase activity was stimulated 160-fold by the ribosomal particle (Daigle and Brown, 2004; Himeno *et al*., 2004). YjeQ bound the mature 30S subunit tightly in the presence of GMP-PNP (non-hydrolyzable analog of GTP) and minimally with GDP (Daigle and Brown, 2004). However, YjeQ demonstrated weak binding and stimulation of GTPase activity in the presence with the immature 30S subunit (Goto *et al*., 2011; Himeno *et al*., 2004). The addition of excess YjeQ to the 70S particles caused it to dissociate into 30S and 50S subunits (Himeno *et al*., 2004). This suggested that YjeQ acts in the very last steps of ribosomal assembly, where it is released in a nucleotide-dependent manner upon maturation of the 30S subunit.

YjeQ is found in Gram-negative bacteria such as *Escherichia coli, Salmonella typhimurium and Thermotoga maritima* and its homologue YloQ in Gram-positive bacteria such as *Bacillus subtilis*. The structure is well conserved across bacteria and is comprised of three domains; an N-terminal OB-fold, a central GTPase and a C-terminal zinc-finger domain (Levdikov *et al*., 2004; Nichols *et al*., 2007; Shin *et al*., 2004). There is no crystal structure of the *E. coli*

YjeQ that has been solved however the structure of the *S. typhimurium* YjeQ is solved and shares 92% sequence identity and 94% sequence similarity. Therefore conclusions on the *E. coli* YjeQ structure have been derived from the well-conserved structure of *S. typhimurium* YjeQ (Figure 2).

In the crystal structures of YjeQ the three domains are observed. In the sequence of YjeQ there is an additional region at the N-termini, RID (Ribosome Interaction Domain), which is disordered and not solved in the crystal structures (Levdikov *et al*., 2004; Nichols *et al*., 2007; Shin *et al*., 2004). This region was found to be required for tight binding to the 30S ribosome in *E. coli* YjeQ (Daigle and Brown, 2004). Interestingly, this region is sometimes found to be cleaved off by contaminating proteases in ribosome preparations or when YjeQ is overexpressed in the cell without an N-terminal histidine tag (Daigle *et al*., 2002). Proceeding the RID is the OB-fold domain (Oligosaccharide-binding), which is essential for YjeQ binding to the 30S subunit and 30S subunit-dependent GTP hydrolysis (Daigle and Brown, 2004). The OB-fold consists of antiparallel β-sheets that come together to form a β-barrel (Shin *et al*., 2004). Typically, this domain is found in proteins that bind nucleic acids, particularly single-stranded or unusually folded nucleic acids (Theobald *et al*., 2003).

The central domain consists of a circularly permutated GTPase domain which is unique to a class of GTPases that have a role in RNA-binding (Anand *et al*., 2006). The GTPase domain primarily consists of a six-stranded ß-sheet (Nichols *et al*., 2007). The overall folding of the domain is characteristic of a

Rossman fold, which resembles the GTPase domain of proteins in the TRAFAC family (Shin *et al*., 2004). The TRAFAC family of GTPases consists of proteins involved in translation, signal transduction, cell motility and intracellular transport. The circular permutation found in the GTPase domain has an unusual order of the five GTPase loops. Instead of being G1-G2-G3-G4-G5 pattern that is typically observed (Leipe *et al*., 2002), it consists of a G4-G5-G1-G2-G3 pattern (Shin *et al*., 2004). This permutation causes the switch I and switch II regions of the GTPase domain that coordinate GTP binding and hydrolysis to be further downstream of the domain. This may be the reason circularly permutated GTPases have a c-terminal domain to anchor the c-terminal end of the GTPase domain or possibly have a critical role on the effector molecule, in this case the RNA (Anand *et al*., 2006). Interestingly, the switch II region of YjeQ is found located in the connecting loop between the GTPase domain and the C-terminal zinc-finger domain (Shin *et al*., 2004). This suggests there may be a direct mechanical effect on the C-terminal zinc-finger domain upon GTP hydrolysis.

The C-terminal zinc-finger domain has a unique zinc-binding motif (Shin *et al*., 2004) that most closely resembles a combination of a TAZ2 domain-like fold and a short zinc-binding loop (Krishna *et al*., 2003). Two of the cysteines and one histidine that coordinate the zinc ion are located in the loop connecting two α-helices, while the fourth cysteine is located at the start of the second α-helix of the domain. Zinc-finger motifs are often required for structural integrity of protein folding and/or to bind DNA or RNA. Although the YjeQ zinc-finger motif is unique

to YjeQ, a DALI database search revealed it had close structural similarity to a portion of DNA repair protein, Rad51 (Shin *et al*., 2004). However, this domain was not a zinc-finger domain. Beyond the zinc-finger motif is a helical extension that has been referred to as the c-terminal extension (CTE), seen in Figure 2A (Nichols *et al*., 2007). Whether this has a function unique to the zinc-finger domain is unclear, since it is not directly required to coordinate the zinc ion.

1.5 YjeQ and assembly of the 30S subunit

The structure of YjeQ from different bacterial species has been determined and the GTPase activity of the protein alone and in the presence of the ribosome has been well characterized. However, the function of the protein in regards to how it helps the 30S subunit become mature and functional is poorly understood. The insights into possible function of YjeQ have largely come from structural studies on the 30S subunit produced under YjeQ deficient conditions or in the presence of YjeQ (Guo *et al*., 2011; Jomaa *et al*., 2011a; Jomaa *et al*., 2011b; Kimura *et al*., 2008), as has also been done with other assembly factors (Clatterbuck Soper *et al*., 2013; Datta *et al*., 2007; Guo *et al*., 2013; Leong *et al*., 2013; Sharma *et al*., 2005).

The Δ*yjeQ* strain of *E. coli* was the first assembly factor to be used as a tool to gain insight into the direct effect of assembly factors on 30S subunit assembly The immature 30S subunit produced from Δ *yjeQ* cells was analyzed for structural differences from the mature 30S subunit of wild-type cells using cryo-EM (Figure 3A) (Jomaa *et al*., 2011a).

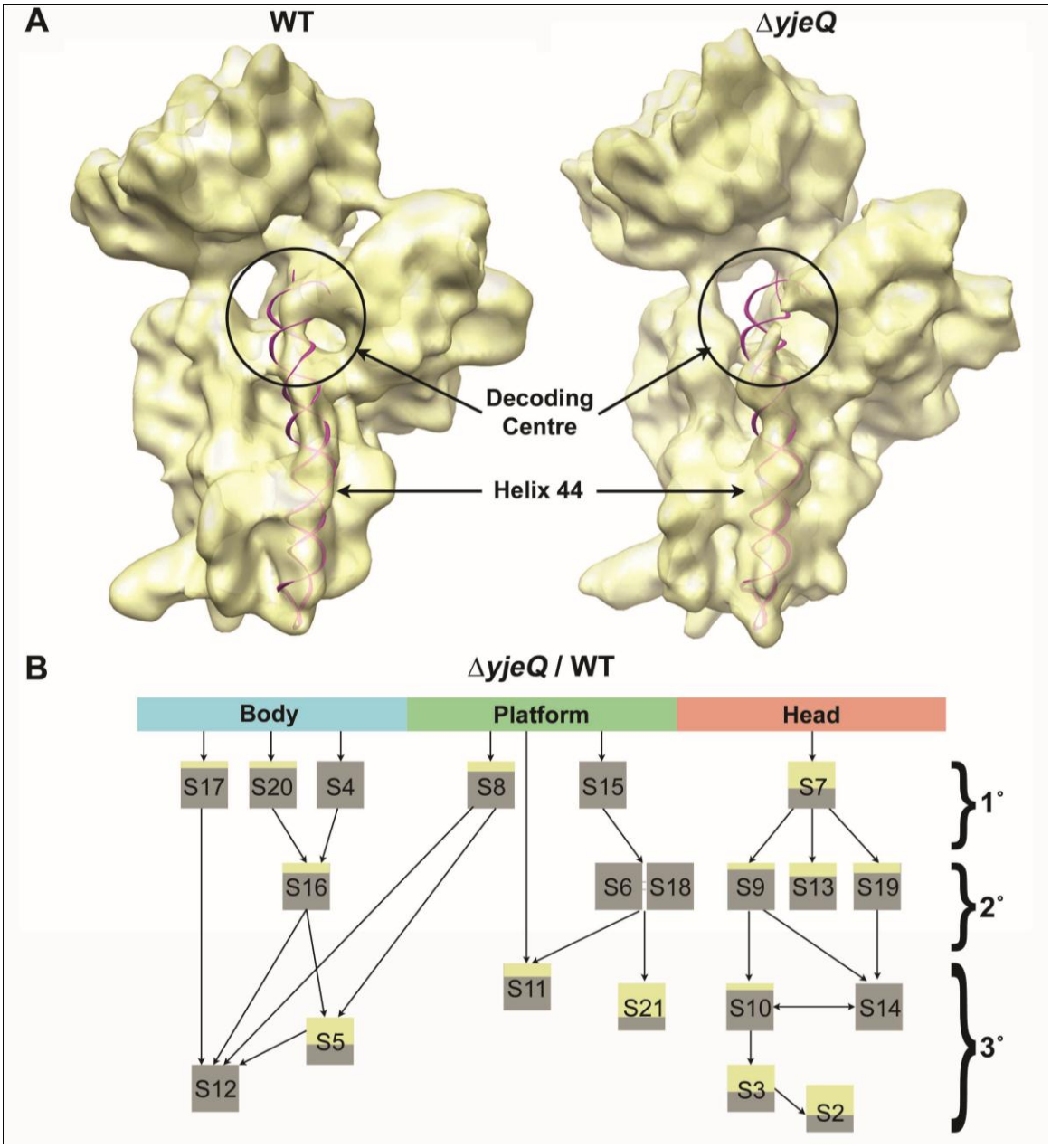

Figure 3. The immature 30S subunit from Δ *yjeQ E. coli*. The immature 30S subunit was obtained from cells that have a deletion of the *yjeQ* gene. (A) The cryo-EM structure of the immature 30S subunit (right) compared to the mature 30S subunit (left) shows a missing density for the top of h44, as indicated by the docked x-ray structure of h44 (magenta). The remainder of the 30S subunit from the crystal structure was excluded in this figure. (EMDB 1774 fitted with PDB 2AVY) (B) A modified Nomura-map of the hierarchal ribosomal protein binding to the 16S rRNA (Jomaa et al., 2011a) depicts the primary (1˚), secondary (2˚) and tertiary (3˚) proteins. Each box represents the degree of underrepresentation of the R-protein in Δ*yjeQ*/WT cells, shaded in yellow.

The protein content of both mature and immature 30S subunits was analyzed using mass spectrometry iTRAQ analysis. This revealed that the immature 30S particles from Δ*yjeQ* cells had a greater under-representation of ribosomal proteins S21, S1 and S2 compared to mature 30S particles and a majority of the ribosomal protein content was unchanged (Figure 3B). This implicated YjeQ in late stages of ribosome assembly since S21 and S2 are late binding ribosomal proteins and S1 typically falls off during ribosomal preparation (Held *et al*., 1974). The overall structure of the 30S subunit remained intact except for one key exception. The decoding centre, particularly h44, was flexible and following averaging no density was observed for the helix (Figure 3). This indicated that the conformation of the decoding centre was not formed and functional in the immature particle.

The deletion of YjeQ revealed a distortion of the decoding centre that was also the binding site of YjeQ to the 30S subunit. The location of YjeQ bound to the 30S subunit was shown through chemical foot printing and cryo-EM studies (Guo *et al*., 2011; Jomaa *et al*., 2011b; Kimura *et al*., 2008). These studies revealed that YjeQ interacts with the decoding centre of the 16S rRNA and sits between the head and platform domains of the 30S subunit. Two cryo-EM structures of the mature 30S subunit with YjeQ from *E. coli* placed YjeQ in the same position, however the structures revealed two potential orientations of YjeQ when bound to the 30S subunit (Guo *et al*., 2011; Jomaa *et al*., 2011b).

One structure showed YjeQ bound with the orientation in which the N-terminal OB-fold of YjeQ interacted with the head of the 30S subunit and the C-terminal zinc-finger interacted with h44 (Figure 4A) (Jomaa *et al*., 2011b). The C-terminal domain appeared to clash with the density of what should be h44 and may have caused a displacement of the top of h44, which resulted in a missing density in the cryo-EM map. The second structure showed the N-terminal OB-fold domain of YjeQ interacted with h44 and no displacement of the helix, while the C-terminal zinc-finger domain interacted with the head of the 30S subunit (Guo *et al*., 2011). Although the orientations of YjeQ differ in both structures, the placement of YjeQ in both cryo-EM structures were in agreement with chemical foot printing studies (Kimura *et al*., 2008). The binding site of YjeQ partially overlapped with that of translation factors, IF2 and IF3, as well as the inter-subunit bridges (B3, B2a and B7a) that bind the 30S and 50S subunits. This explained why in previous studies excess amounts of YjeQ with GDPNP (non-hydrolyzable analog of GTP) caused the 70S subunit to dissociate (Himeno *et al*., 2004).

1.6 Interplay of YjeQ and RbfA

One of the proposed functions to date of YjeQ is that its role in ribosomal assembly is to cause the removal of RbfA from the mature 30S subunit (Goto *et al*., 2011).

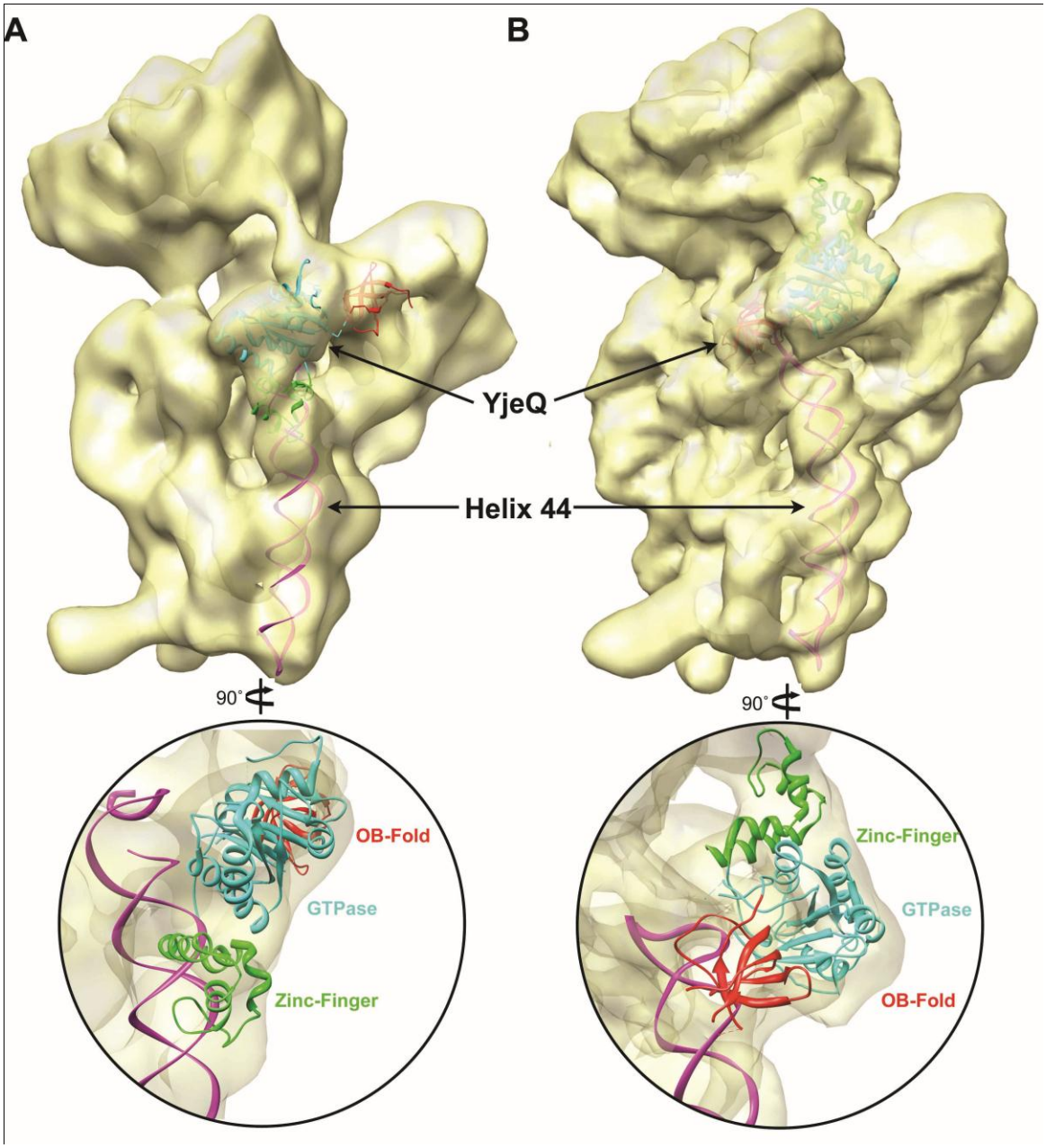

Figure 4. Complex of *E. coli* YjeQ with 30S subunit. The cryo-EM complexes of YjeQ binding to the mature 30S subunit from wild type cells. (A) Complex from Ortega group fitted with h44 and the YjeQ crystal structure. Zoom in view below shows displacement of h44 and interaction with zinc-finger domain of YjeQ. (EMDB 1895 fitted with PDB 4a2i) (B) Complex from the Gao group fitted with h44 and YjeQ crystal structure. Zoom in view below shows the OB-fold domain of YjeQ wrapped around h44 and no displacement is observed. (EMDB 1884 fitted with PDB 2YKR)

Rbfa is a ribosomal maturation factor whose absence resulted in a cold-sensitive phenotype, decreased growth rate of cells and an accumulation of free immature 30S subunits (Bylund *et al*., 1998; Dammel and Noller, 1995; Xia *et al*., 2003). RbfA is also unique among the other assembly factors because it is a cold-shock protein. During cold-shock, RbfA was upregulated and bound to the 30S subunit (Jones and Inouye, 1996). The complex of RbfA with the 30S subunit from *Thermus thermophilus* revealed that RbfA bound in the cleft behind the head and the platform of the 30S subunit located behind the decoding centre (Figure 5) (Datta *et al*., 2007). Extra densities were observed protruding around the placement of RbfA, which were suggested to be displacement of portions of helices 44 and 45. The functional role of RbfA in 30S subunit assembly has not yet been revealed, but mutations of RbfA suggest that it is removed by YjeQ in a nucleotide-dependent manner (Goto *et al*., 2011). These experiments showed that a mutation that decreases the affinity of RbfA for the 30S subunit was able to rescue the defects associated with the Δ*yjeQ* strain. When RbfA was bound to the mature 30S subunit, it was removed by YjeQ in the presence of GTP or GDPNP (non-hydrolyzable GTP). However, YjeQ was unable to remove RbfA bound to the immature 30S subunit from a Δ*yjeQ*Δ*rbfA* double-knockout strain of *E. coli*.

The interplay between YjeQ and RbfA is the first biochemical link shown between assembly factors that demonstrate that these proteins function together.

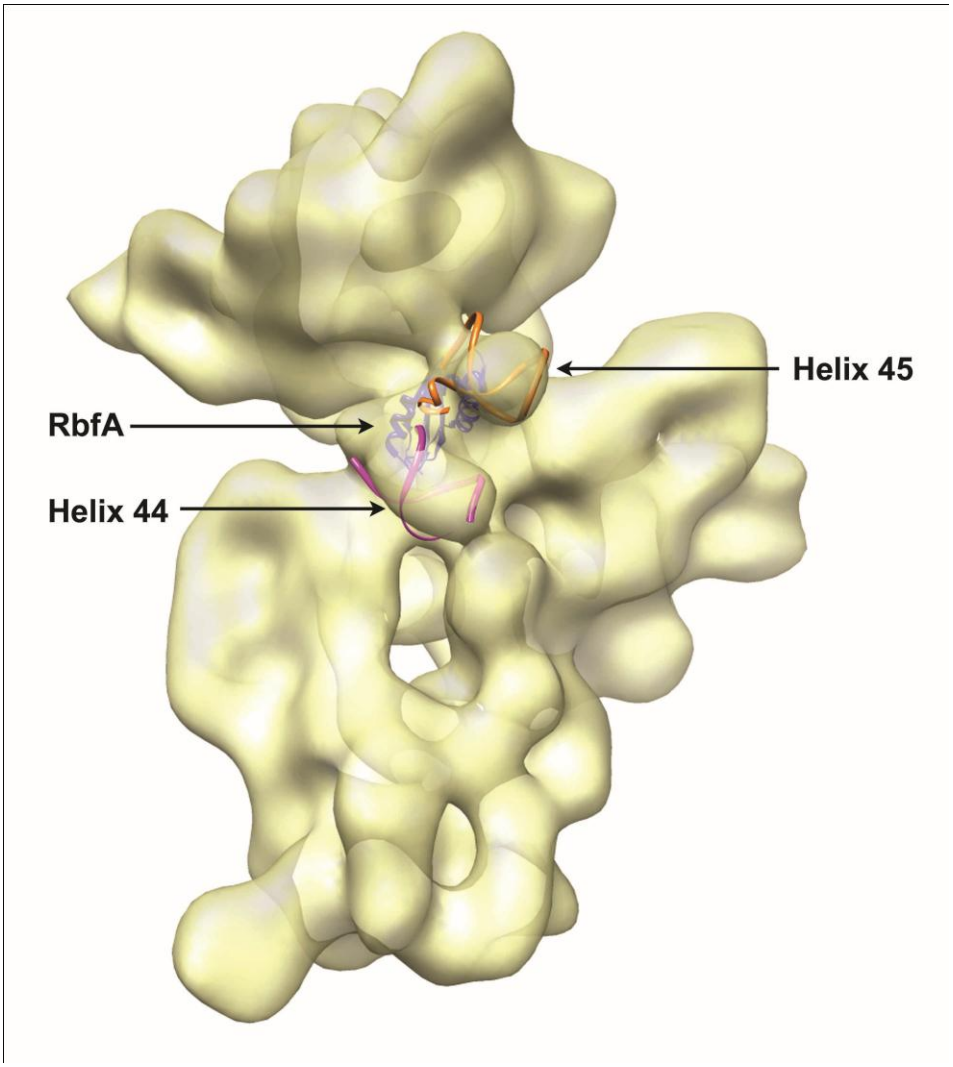

Figure 5. Structure of the complex of RbfA with the 30S subunit. The complex is formed from the mature 30S subunit and RbfA from Thermus thermophilus. The RbfA (blue) binds in the neck of the 30S subunit and appears to cause a displacement of a portion of h44 (magenta) and h45 (orange) out towards the interface. (EMDB 1413 fitted with PDB 2R1C and PDB 2R1G).

However it has not yet been revealed how these assembly factors cause the maturation of the 30S subunit, only that they are involved in the process. Analysis of existing cryo-EM structures revealled that the decoding centre is the main site of structural changes when both proteins were individually bound to the 30S subunit (Datta *et al*., 2007; Jomaa *et al*., 2011b). YjeQ appears to distort the

top of h44 in a manner that would be incompatible with the binding site of RbfA. It may be performing this function through its C-terminal zinc-finger domain that has not yet been characterized. One option is that following maturation of the 30S subunit, YjeQ binds and hydrolyzes GTP causing a downstream shift of its C-terminal domain. This conformational change may in turn cause a displacement of the top of h44 and removal of RbfA. The second option is that YjeQ binds to a nearly mature 30S subunit that is also bound by other assembly factors, such as RbfA. Upon maturation and stable conformation of h44, the C-terminal zinc-finger domain may be induced to shift, causing an upstream activation of the GTPase domain and release of YjeQ.

Here we use C-terminal variants of YjeQ to assess the function of YjeQ in 30S subunit maturation. The variants demonstrated that YjeQ requires the zinc-finger domain to bind tightly to that 30S subunit. However, the C-terminal extension of YjeQ is not necessary for binding to the 30S subunit but is required for 30S subunit-dependent GTP hydrolysis. This extension, which interacts with h44 when bound to the 30S subunit, is also required to remove RbfA from the mature particle. This data suggests that YjeQ acts as a checkpoint protein that is signaled to release from the 30S subunit once the decoding centre is in a mature conformation. The interplay between RbfA and YjeQ is likely coordinated around the maturation of the decoding centre. The proteins remain bound until the decoding centre is nearly mature, at which point RbfA is no longer compatible to bind the 30S subunit. Following removal of all assembly factors and complete

maturation of the decoding centre, YjeQ would be signaled to hydrolyze GTP and release from the 30S subunit. This work provides insight into the mechanism of interplay between these two assembly factors. With the help of additional assembly factors, YjeQ and RbfA are involved in stabilizing the decoding centre into a mature conformation. Understanding the mechanism behind the maturation of the decoding centre and the role of each individual assembly factor in this process will help provide a clear picture of the late stages of 30S subunit biogenesis.

2. MATERIALS AND METHODS

2.1 Cell lines and protein constructs

The *Escherichia coli* wild type (BW25113) and Δ*yjeQ* cells were provided by Dr. E. Brown (McMaster University) that were originally obtained from the Keio collection containing single-gene deletions (Baba *et al*., 2006).

The pDEST17:*yjeQ* plasmid was provided from Dr. E. Brown (McMaster University) and prepared by Gateway Recombination Cloning technology (Invitrogren) (Daigle *et al*., 2002). The YjeQ mutant constructs were constructed using QuikChange® II XL Site-Directed Mutagenesis Kit (Agilent Technologies). The corresponding primer sets used for mutagenesis of pDEST17:*yjeQ* into pDEST17:*m1*, pDEST17:*m2*, pDEST17:*m3* and pDEST17:*m4* are listed in Table 1. Mutations were verified by sequencing (MOBIX, McMaster University).

Table 1. YjeQ C-terminal variant mutagenesis primers

YjeQ Variants	Name of Primer	Primer sequence (5'-3')
M1	M1 Fwd	GTTCGGCCTCTGGCACTGAGAGCCGGAACAAATCAC
	M1 Rev	GTGATTTGTTCCGGCTCTCAGTGCCAGAGGCCGAAC
M2	M2 Fwd	CCGGAACAAATCACTCAGGGCTGAGTCGAATTCCATGAC
	M2 Rev	GTCATGGAATTCGACTCAGCCCTGAGTGATTTGTTCCGG
M3	M3 Fwd	GAAGCGGTTGAGGAAGGGTAAATCGCGGAAACCCGTTTC
	M3 Rev	GAAACGGGTTTCCGCGATTTACCCTTCCTCAACCGCTTC
M4	M4 Fwd	CCATGACTATTTAGGTCTGTGTGCATATGCCGATTGCAAACACG
	M4 Rev	CGTGTTTGCAATCGGCATATGCACACAGACCTAAATAGTCATGG
$M3^A$	$M3^A$ Fwd	GCGGTTGAGGAAGGGTGAATCGCGGAAACCCG
	$M3^A$ Rev	CGGGTTTCCGCGATTCACCCTTCCTCAACCGC

** Underlined sequence indicates triplet codon that was mutated*

The pCA24N and pCA24N:*yjeQ* plasmids were provided from Dr. E. Brown (McMaster University) that were originally obtained from the ASKA library

(Kitagawa *et al*., 2005). The pCA24N:*m3*^{A} plasmid was constructed from pCA24N:*yjeQ* using QuikChange® II XL Site-Directed Mutagenesis Kit (Agilent Technologies). Corresponding primers used in mutagenesis are listed in Table 1. Mutations were verified by sequencing (MOBIX, McMaster University).

The pMAT:*rbfA* plasmid was obtained by gene synthesis (GeneArt®, Life Technologies). The *rbfA* gene with an N-terminal His_6-tag was excised from the pMAT vector by restriction digests using NdeI and BamHI-HF restriction enzymes. The gene was ligated into pET15b and the presence of the gene was verified by restriction digestion and sequencing (MOBIX, McMaster University).

2.2 Purification of YjeQ and YjeQ variants

YjeQ, M1, M2, M3 and M4 were expressed with an N-terminal His_6-tag in *E. coli* BL21-A1 cells that were transformed with pDEST17:*yjeQ,* pDEST17:*m1*, pDEST17:*m2*, pDEST17:*m3* and pDEST17:*m4* respectively. One litre of cells were grown in LB medium at 37°C to OD_{600} of 0.6 and then induced with 0.2% L-arabinose. YjeQ and M4 were induced for 3 hours at 37°C, while M1, M2 and M3 were induced for 16 hours at 16°C due to low solubility of proteins at 37°C. All cells were harvested after induction by centrifugation at 8,500*g* for 15 min. The cell pellets were then washed with 1X PBS buffer (137 mM NaCl, 2.7 mM KCl, 8.1 mM Na_2HPO_4, 1.76 mM KH_2PO_4 at pH 7.4), centrifuged at 1,400*g* for 20 minutes and resuspended in 20 mL of lysis buffer (50 mM Tris-HCl at pH 8.0, 10% [w/v] sucrose, 100 mM NaCl). The cell suspension was lysed by passing it through the French press three consecutive times at 20,000 lb/in^2. Lysate was

separated from cell debris by centrifugation at 30,000*g* for 40 mins and NaCl was added to clarified lysate to bring it to 0.5 M. The Lysate was then filtered with a 0.45-µm filter and loaded onto a HiTrap Metal Chelating column (GE Healthcare Life Sciences) charged with Ni^{2+} and equilibrated with 50 mM Tris-HCl at pH 8.0, 0.5 M NaCl and 5% [v/v] glycerol. The column was washed with 45 mM and 90 mM imidazole and proteins were eluted with 240 mM imidazole. The purity of fractions were monitored by 15% SDS-PAGE. Fractions with pure protein were collected and dialyzed overnight at 4°C against buffer containing 50 mM Tris-HCl at pH 8.0 and 5% [v/v] glycerol. For M1, M2 and M3, dialysis buffer also included 120 mM NaCl to increase protein solubility.

The N-terminal His_6-tag was removed by digestion with purified tobacco etch virus (TEV) protease during the previous overnight dialysis step. To this end 0.05 mg of TEV protease per milligram of YjeQ were added to the pooled fractions. Following digestion and dialysis, the reaction was loaded onto the HiTrap Metal Chelating column (GE Healthcare Life Sciences) charged with Ni^{2+} and equilibrated with 50 mM Tris-HCl at pH 8.0, 60 mM imidazole, 0.2 M NaCl and 5% [v/v] glycerol. The flow through containing the untagged protein was recovered and purity of fractions showing cleaved protein was monitored by 15% SDS-PAGE. Fractions with pure, cleaved protein were dialyzed overnight at 4°C against buffer containing 50 mM Tris-HCl at pH 8.0 and 5% [v/v] glycerol. For M1, M2 and M3, dialysis buffer also included 120 mM NaCl. Pure protein was

concentrated using a 10 kDa-cutoff filter (Amicon). The protein was frozen in liquid nitrogen and stored at -80°C.

2.3 Purification of RbfA

RbfA was expressed with an N-terminal His_6-tag in *E. coli* BL21-DE3 cells that were transformed with pET15b:*rbfA*. One litre of cells were grown in LB medium at 37°C to OD_{600} of 0.6 and then induced with 1 mM Isopropyl β-D-1-thiogalactopyranoside (IPTG) for 3 hours at 37°C. Following induction, cells were harvested by centrifugation at 8,500*g* for 15 min. The cell pellet was then washed with 1X PBS buffer (137 mM NaCl, 2.7 mM KCl, 8.1 mM Na_2HPO_4, 1.76 mM KH_2PO_4 at pH 7.4), centrifuged at 1,400*g* for 20 minutes and resuspended in 20 mL of lysis buffer (50 mM Tris-HCl at pH 8.0, 10% [w/v] sucrose, 100 mM NaCl). The cell suspension was lysed by passing it through the French press three consecutive times at 20,000 lb/in^2. Lysate was separated from cell debris by centrifugation at 30,000*g* for 40 mins and NaCl was added to clarified lysate to bring it to 0.5 M. The Lysate was then filtered with a 0.45-µm filter and loaded onto a HiTrap Metal Chelating column (GE Healthcare Life Sciences) charged with Ni^{2+} and equilibrated with 50 mM Tris-HCl at pH 8.0, 0.5 M NaCl and 5% [v/v] glycerol. The column was washed with 30 and 75 mM imidazole, and proteins were eluted with 240 mM imidazole. Purity of fractions was monitored by 15% SDS-PAGE. Fractions with nearly pure RbfA were collected and dialyzed overnight at 4°C against buffer containing 50 mM Tris-HCl at pH 8.0 and 5% [v/v] glycerol.

Dialyzed protein was loaded onto a HiTrap Q HP Anion Exchange column (GE Healthcare Life Sciences) that was equilibrated with 50 mM Tris-HCl at pH 8.0 and 10% [v/v] glycerol. The column was washed with the same buffer containing 50 mM NaCl and eluted by increasing the concentration of the NaCl in the buffer to 100 mM NaCl. Purity of the fractions was monitored by 15% SDS-PAGE. Fractions with pure RbfA were dialyzed overnight at 4°C against buffer containing 50 mM Tris-HCl at pH 8.0 and 5% [v/v] glycerol and concentrated using a 10 kDa-cutoff filter (Amicon). The protein was frozen in liquid nitrogen and stored at -80°C. This His-tag of RbfA (18 kDa) was not removed from the protein in order to allow the RbfA (15 kDa) band to be viewed individually in the presence of 30S ribosomal proteins in 15% SDS-PAGE (see Results).

2.4 Purification of ribosome particles

The wild type (BW25113) and Δ*yjeQ E. coli* strains were prepared following previously described methods (Daigle *et al*., 2002; Jomaa *et al*., 2011a). One litre of each strain was grown at 37°C to an OD_{600} of 0.6 (wild type) and 0.2 (Δ*yjeQ*). The following steps were all performed at 4°C.

Cells were harvested by centrifugation at 8,500*g* for 15 min. The cell pellet was resuspended in Buffer A (20 mM Tris-HCl at pH 7.5, 10.5 mM magnesium acetate, 100 mM NH_4Cl, 0.5 mM EDTA and 3 mM ß-mercaptoethanol). Following resuspension, three consecutive passes through the French Press at 20,000 lb/in^2 was used to lyse cells. The lysate was centrifuged at 30,000*g* for 40 min to remove cell debris. The supernatant was

laid over an equal volume of 1.1 M sucrose cushion made with Buffer B (20 mM Tris-HCl at pH 7.5, 10.5 mM magnesium acetate, 500 mM NH_4Cl, 0.5 mM EDTA and 3 mM ß-mercaptoethanol) and centrifuged 100,000*g* for 16 hr. The ribosomal pellet was gently washed by resuspension in Buffer C (10 mM Tris-HCl at pH 7.5, 10.5 mM magnesium acetate, 500 mM NH_4Cl, 0.5 mM EDTA and 2 mM ß-mercaptoethanol). Following resuspension, the crude ribosomes were pelleted by centrifugation at 100,000*g* for 16 hr.

Ribosomal subunits from wild type *E. coli* were obtained by resuspending the crude ribosome pellet in Buffer F (10 mM Tris-HCl at pH 7.5, 1.1 mM magnesium acetate, 60 mM NH_4Cl, 0.5 mM EDTA and 2 mM ß-mercaptoethanol) (disassociating conditions). While ribosomal subunits from Δ*yjeQ E. coli* were resuspended in Buffer E (10 mM Tris-HCl at pH 7.5, 10 mM magnesium acetate, 60 mM NH_4Cl and 3 mM ß-mercaptoethanol) (associating conditions). To separate the 30S, 50S and 70S (associating conditions only) subunits in both ribosomal preparations, 120 A_{260} units of ribosome were layered onto a 32 mL 10-30% [wt/vol] sucrose gradient. The sucrose gradient was made with Buffer F or E, corresponding to the buffer used to resuspend the crude ribosomal pellet. The gradients were centrifuged at 43,000*g* for 16 hr using a Beckman SW32 Ti swinging-bucket rotor. Gradients were then fractioned using an AKTAprime purification system (GE Healthcare). The elution peaks of the ribosomal subunits were monitored by absorbance at A_{260}. Purified ribosomal subunits were obtained by centrifugation at 100,000*g* for 16 hr and pellets of 30S, 50S and 70S

subunits were resuspended in Buffer E. Purified subunits were frozen in liquid nitrogen and stored at -80°C. Purity of ribosomal subunits was analyzed by extracting rRNA from approximately 10-50 pmoles of ribosome with the RNeasy Mini Kit (Qiagen). Concentration of purified rRNA was measured by absorbance at A_{260}, where 1 absorbance unit was equivalent to 40 µg/mL of RNA. Approximately 0.8 µg of purified rRNA was loaded on a 0.9% synergel - 0.7% agarose gel, using methods described previously to separate 23S, 17S, and 16S rRNA (Wachi *et al*., 1999).

2.5 Circular dichroism for YjeQ folding analysis

Circular dichroism (CD) Spectroscopy was used to assess the secondary folding of YjeQ mutants, M1, M2, M3 and M4, in comparison with wild type YjeQ. CD spectra for each YjeQ protein were collected using a Circular Dichroism Spectrometer Model 410 (Aviv Biomedical Inc.). Spectral scans were performed from 260 to 200 nm, with step resolution of 1.0 nm and bandwidth of 1.0 nm. A 1-mm-path-length quartz cuvette was used for the measurements. Scans were performed three consecutive times for each protein at 4°C, 16°C, 25°C and 37°C within a 15 min incubation. Protein samples were prepared in Binding Buffer 300 (10 mM Tris-HCl at pH 8.0, 7 mM magnesium acetate, 300 mM NH_4Cl and 1 mM dithiothreitol (DTT)) at 0.5 mg/mL. The molar ellipicity [θ] [$deg*cm^2*dmol^{-1}$] was calculated and plotted for the CD spectra analysis.

Instability of the YjeQ mutants was also assessed by incubation of the proteins at three temperatures: 4°C, 16°C and 37°C and two salt concentrations

(60 mM NH_4Cl and 300 mM NH_4Cl). YjeQ and YjeQ mutants were incubated at the various temperatures for 15 min in Binding Buffer 60 (10 mM Tris-HCl at pH 8.0, 7 mM magnesium acetate, 60 mM NH_4Cl and 1 mM DTT) and Binding Buffer 300 (10 mM Tris-HCl at pH 8.0, 7 mM magnesium acetate, 300 mM NH_4Cl and 1 mM DTT). Following incubation, protein samples were centrifuged at 12,000*g* for 5 min and the non-precipitated fraction of the protein was estimated by resolving the supernatant by 15% SDS-PAGE.

2.6 Binding assays

Reactions for filtration assays were prepared by mixing 200 pmoles of protein (YjeQ, YjeQ variants and/or RbfA) with 40 pmoles of 30S subunit in a 100 µL reaction in either Binding Buffer 60 (10 mM Tris-HCl at pH 8.0, 7 mM magnesium acetate, 60 mM NH_4Cl, 1 mM DTT and 1 mM GMP-PNP) or Binding Buffer 300 (10 mM Tris-HCl at pH 8.0, 7 mM magnesium acetate, 300 mM NH_4Cl, 1 mM DTT and 1mM GMP-PNP). The concentration of each protein assembly factor in this reaction was five-fold that of the ribosomal particle. Nucelotide GMP-PNP was only added in reactions containing YjeQ and YjeQ variants. Reactions were incubated at 16°C, 25°C or 37°C for 15 min followed by centrifugation in a 100 kDa Nanosep® Centrifugal Devices (PALL). In cases where YjeQ was added following a 15 min incubation of RbfA with the ribosomal particle, the binding reaction was allowed to proceed for another 15 min. Reactions containing RbfA were not allowed in any case to proceed past 30 min, as previous studies have shown that this protein falls off from the mature 30S

subunit with time (Goto *et al*., 2011). Prior to loading the binding reactions in the 100 kDA Nanosep® Centrifugal Devices (PALL), its filter membrane was blocked by loading 500 µL of 1% [w/v] BSA and washed twice with 500 µL of RNAse Free water. Reactions were spun for 12,000*g* for 10 min to separate 30S particles and 30S-bound proteins that were retained by the filter from unbound proteins in flow-through (FT). The flow-through was collected and the filter was washed gently twice with 100 µL of Binding Buffer 60 or 300 followed by a 5 min spin at 12,000*g*. Finally, the 30S particles and 30S-bound proteins retained by the filter were vigorously resuspended in 100 µL of Binding Buffer 60 or 300 and collected as the bound fraction (B). To resolve the flow-through and bound fractions, 30 µL of sample mixed with 6X SDS-PAGE sample loading buffer were loaded onto a 4-12% Criterion^{TM} XT Bis-tris gel (Bio-Rad). Samples were run in XT MOPS buffer (Bio-Rad).

In the case of the pelleting assays, reactions were prepared by mixing 250 pmoles of protein (YjeQ, YjeQ variants and/or RbfA) with 50 pmoles of 30S particle in a 50 µL reaction in either Binding Buffer 60 or Binding Buffer 300. The final concentration of GMP-PNP in the binding reactions containing YjeQ and YjeQ variants was 2 mM. The concentration of each protein assembly factor in this reaction was five-fold that of the ribosomal particle. In cases where RbfA was added following a 15 min incubation of YjeQ with the ribosomal particle, the binding reaction was allowed to proceed for another 15 min. Reactions were carried out at 16°C or 25°C. Following incubation, reactions were laid over a 150

µL 1.1 M sucrose cushion in either Binding Buffer 60 or 300 and spun for 250,000*g* for 5 hr. The supernatant (S) containing free protein that did not pellet with the 30S subunits was collected. The pellet (P) containing the 30S particles and 30S-bound proteins was resuspended in 200 µL of Binding Buffer 60 or 300. To resolve the supernatant and pellet fractions, 30 µL of sample mixed with 6X SDS-PAGE sample loading buffer were loaded onto a 4-12% Criterion^{TM} XT Bis-tris gel (Bio-Rad). Samples were run in XT MOPS buffer (Bio-Rad).

2.7 GTPase activity assays

The intrinsic GTP hydrolysis rate of YjeQ, M1, M2, M3 and M4 variants was measured by incubating each protein (100 nM) with GTP (250 µM) at 25°C for 60 min and then measuring the release of free phosphate using the Malachite Green Phosphate Assay Kit (BioAssay Systems). The reactions were initiated by adding GTP to proteins in reaction buffer containing 10 mM Tris-HCl at pH 8.0, 7 mM magnesium acetate, 300 mM NH_4Cl and 1 mM DTT. In those cases where the stimulation of GTPase activity of YjeQ or YjeQ variants by the 30S particles were measured, the sample also contained 100 nM of 30S particle before GTP was added. Volume of the reactions was 80 µL. Reactions were terminated by addition of 20 µL of the malachite green reagent and an additional incubation of 15 min at 25°C before monitoring color formation by measuring absorbance at 620 nm. The amount of phosphate produced by the reaction containing only buffer and GTP was considered background and was subtracted from each reaction. Reactions were run in a 96-well plate and readings were done with the

Infinite® M1000 multiplate reader (TECAN). Average and standard deviation values were derived from three replicas of each reaction. The amount of free phosphate produced in these reactions was within the linear range of the assay.

2.8 *In vivo* complementation assays

The growth rate of wild-type *ΔyjeQ* and parental (WT) *E. coli* (BW25113) strains was determined by growing the cells at 25°C for 47 hours with shaking. Culture density was monitored by measuring the optical density at 600 nm in a Sunrise™ 96-well plate reader (TECAN) and plotted using Magellan™ (TECAN). Doubling times was calculated according to the formula DT = (t2 − t1)*[log2/(log OD_{600}@t2/log OD_{600}@t1)] and expressed in hours. Growth rates were expressed as k = ln2/DT and expressed in h^{-1}.

The growth curves were produced by inoculating 200 µL of LB media from overnight cultures at 1:100 dilutions. To reintroduce the YjeQ or YjeQ M3 variant, we used the high copy plasmid pCA24N, which expresses the N-terminal histidine-tagged YjeQ under the control of the IPTG-inducible promoter $P_{T5\text{-}lac}$. (see information about these plasmids above). We used standard protocols (Sambrook *et al*., 1989) to transform these plasmids into the *ΔyjeQ* cells before proceeding to obtain the growth curves as described above. In the cultures where we wanted to express YjeQ or the YjeQ M3 variant (or empty pCA24N) plasmid the LB media contained either 1 µM or 100 µM IPTG as specified.

To obtain the ribosome profiles and analyze the rRNA content of these cells, LB cultures (1 L) were grown at 25°C to an OD_{600} of 0.2. In the case of the

strains containing the empty pCA24N plasmid or that encoding for YjeQ or M3 YjeQ variant, we added IPTG to a concentration of 1 µM. Following growth, 10 mL of culture were pelleted by centrifugation at 1,400*g* for 20 min and processed to purify the rRNA. Total rRNA was analyzed by extracting rRNA from the cell pellet with the RNeasy Mini Kit (Qiagen). Concentration of purified rRNA was measured by absorbance at A_{260}, where 1 absorbance unit was equivalent to 40 µg/mL of RNA. Approximately 0.8 µg of purified rRNA was loaded on a 0.9% synergel - 0.7% agarose gel, using methods described previously to separate 23S, 17S, and 16S rRNA (Wachi *et al*., 1999).

The remainder of the cultures was harvested by spinning the cells at 8,500*g* for 15 min to obtain ribosome profiles. Pellets were is washed and resuspended with 20 mL of Buffer A (10 mM Tris-HCl at pH 7.5, 10 mM $MgCl_2$ and 60 mM KCl), divided into three conical tubes and then centrifuged at 1,400*g* for 15 min. Each pellet was resuspended in 6 mL of Lysis buffer (10 mM Tris-HCl at pH 7.5, 10 mM $MgCl_2$ and 60 mM KCl, 0.5 % [v/v] Tween 20, 1 mM DTT, 1 tablet/10 mL cOmplete mini Protease Inhibitor Cocktail (Roche)) and 20 µL of RNAse Free DNAse (Invitrogren). The cell suspension was lysed by passing it through the French press three consecutive times at 20,000 lb/in^2 and clarified by centrifuging at 19,000*g* for 10 min. Ribosomes were pelleted by centrifuging clarified lysate at 125,000*g* for 1 hr 52 min. The ribosomal pellet was rinsed with 1 mL of Buffer B (20 mM Tris-HCl at pH 7.5, 6 mM $MgCl_2$, 30 mM NH_4Cl and 1 mM DTT) and resuspended in 3 mL of Buffer B for 30 minutes on ice. An equal

amount of Buffer C (20 mM Tris-HCl at pH 7.5, 6 mM $MgCl_2$, 800 mM NH_4Cl and 1 mM DTT) was added and further incubated on ice for 1 hr. Ribosomes were clarified by centrifuging 19,000*g* for 10 min and pelleted by centrifuging at 125,000*g* for 1 hr 52 min. The ribosomal pellet was rinsed with 700 µL of Buffer D (20 mM Tris-HCl at pH 7.5, 10 mM $MgCl_2$, 30 mM NH_4Cl and 1mM DTT) (associating buffer) and resuspended in 700 µL buffer D for 1 hr. Crude ribosomes were clarified by centrifuging at 19,000*g* for 10 min and 10 A_{260} units were laid on top of 10-30% sucrose gradients made with Buffer E (20 mM Tris-HCl at pH 7.5, 10 mM $MgCl_2$, 50 mM NH_4Cl and 1 mM DTT). Gradients were centrifuged at 43,000*g* for 16 hr using a Beckman SW41 Ti swinging-bucket rotor. Gradients were then fractioned using an AKTAprime purification system (GE Healthcare). The elution peaks of the ribosomal subunits were monitored by absorbance at A_{260}.

3. RESULTS

3.1 Characterization of YjeQ C-terminal truncation variants

To assess the function of the C-terminal zinc-finger domain of YjeQ, several truncation variants were constructed (Figure 6A). Stop codons were inserted within the zinc-finger domain of a plasmid carrying the YjeQ gene using mutagenesis. The YjeQ M1 variant was constructed with the entire zinc-finger domain removed at the loop connecting the zinc-finger domain to the GTPase domain. The YjeQ M1 variant showed low solubility when purified at 37°C. The loop connecting the zinc-finger domain to the GTPase domain is also partially composed of the switch II region of the GTPase domain and may have resulted in mis-folding of a portion of the GTPase domain (Shin *et al*., 2004). For this reason two more truncation variants were constructed that inserted stop codons immediately before (M2) and after (M3) the helices involved in coordinating the zinc ion. The YjeQ M3 mutant is lacking the C-terminal extension (CTE) identified to be just upstream of the zinc-binding motif. These two mutants also displayed limited solubility at 37°C. To increase the solubility of the C-terminal truncation variants, expression of proteins were induced at 16°C instead of 37°C.

During the purification protocol of the YjeQ C-terminal variants, some precipitation was observed following dialysis. In order to ensure the solubility of proteins following purification, a precipitation test was performed. YjeQ variants were incubated for 15 minutes at 4°C, 16°C or 37°C in low salt (60 mM NH_4Cl) or high salt (300 mM NH_4Cl) buffers.

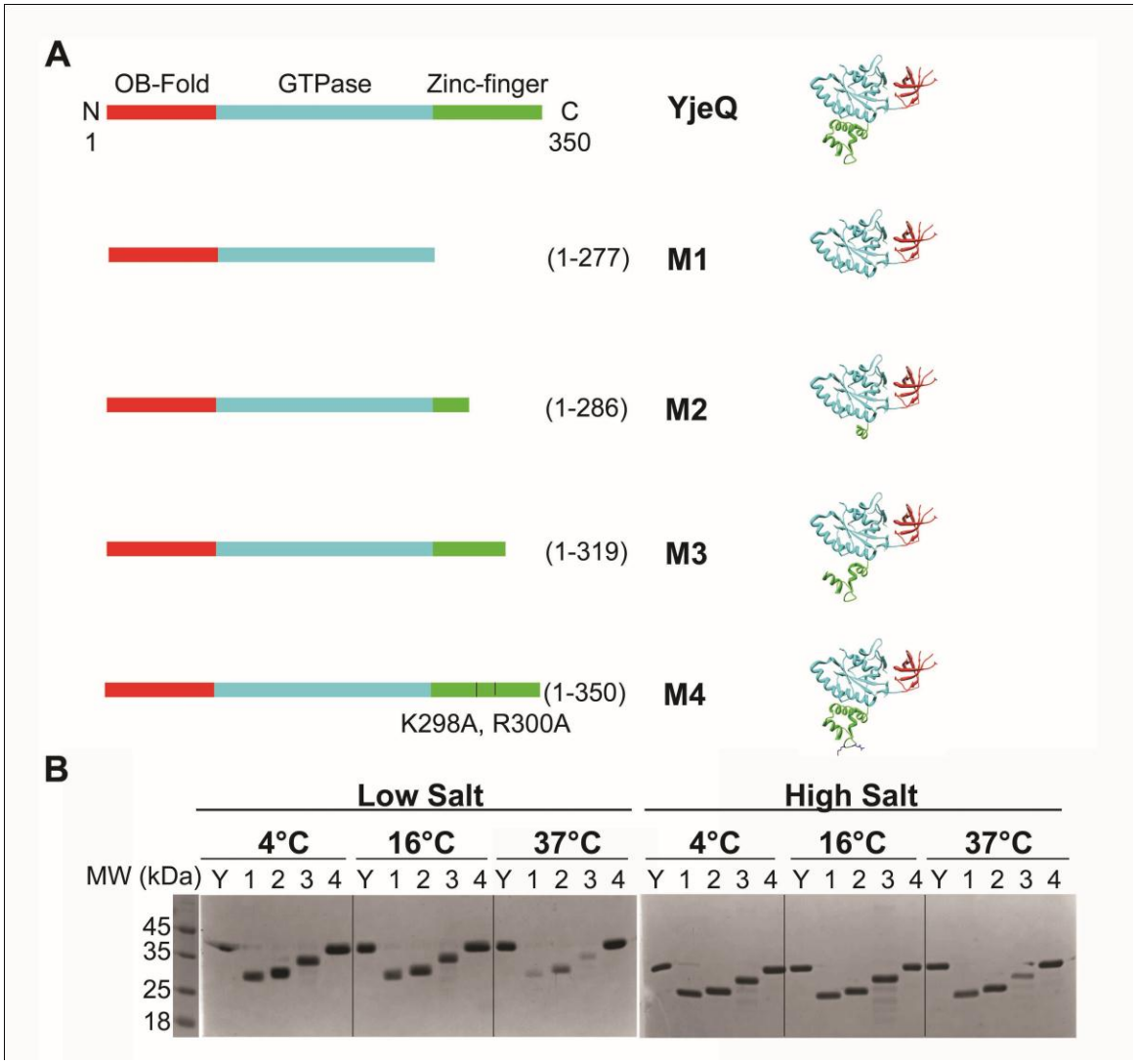

Figure 6. YjeQ C-terminal variants. (A) (Left) Schematic representing truncation of YjeQ at the C-terminal zinc-finger domain for M1, M2, M3 and point mutations for M4. (Right) Modified structure of *S. typhimurium* YjeQ representing YjeQ C-terminal variants made on *E. coli* YjeQ. (PDB 2RCN) (B) Purified YjeQ C-terminal mutants incubated for 15 min at 4°C, 16°C and 37°C in buffer containing low (60 mM NH_4Cl) or high (300 mM NH_4Cl) salt. Samples were spun at 12000*g* for 5 minutes and supernatant that did not precipitate was loaded on 15% SDS-PAGE gel. Lanes are as follows: Y-YjeQ, 1-M1, 2-M2, 3-M3, 4-M4.

This was done to test the stability of the YjeQ C-terminal variants in conditions that would be used for complex formation of YjeQ with the 30S particles.

Following incubation, the samples was spun down at 12,000*g* for 5 min and the non-precipitated fraction of the protein was estimated by resolving the supernatant by 15% SDS-PAGE (Figure 6B). YjeQ variants remained stable after incubation at 4°C and 16°C in both low and high salt buffers. However, when incubation occurred at 37°C in low salt buffer, all three truncation variants (M1, M2 and M3) appeared to be unstable as less soluble protein was observed. This also occurred for M1 and M3 variants in the high salt buffer, but to a much lesser extent. There also appeared to be small amount of degradation products of M3 in all conditions. This could be due to contamination of cellular proteases with M3 purification, as this was observed in repeated purifications of M3 (data not shown). These results showed that increasing temperature of incubation for the YjeQ truncation variants (M1, M2 and M3) led to some instability of proteins, whether incubated in low salt or high salt buffers.

The instability of the YjeQ truncation variants at higher temperatures could be due to a loss of stability of protein folding. As protein folding becomes more unstable and hydrophobic residues are exposed, it is likely that the protein would begin to aggregate and therefore precipitate out of solution. Circular dichroism was used to assess the secondary structural folding of the YjeQ variants compared with YjeQ, which is stable at all temperatures and buffers tested. Circular dichroism uses the output (molar ellipiticy: θ), which is the result of the difference in rotation between left and right circularly polarized light passing through the molecule of interest, to detect presence of secondary structures

(Greenfield, 2006). YjeQ is largely composed of α-helices and antiparallel β-sheets (Nichols *et al*., 2007). Presence of α-helices is detected by negative peaks at 222 nm and 208 nm and a positive peak at 193 nm (Holzwarth and Doty, 1965). Presence of antiparallel β-sheets is detected by negative peaks at 218 nm and positive peaks at 195 nm (Greenfield and Fasman, 1969). YjeQ variants were scanned from 260 nm to 200 nm due to variability of absorbance values outside this range.

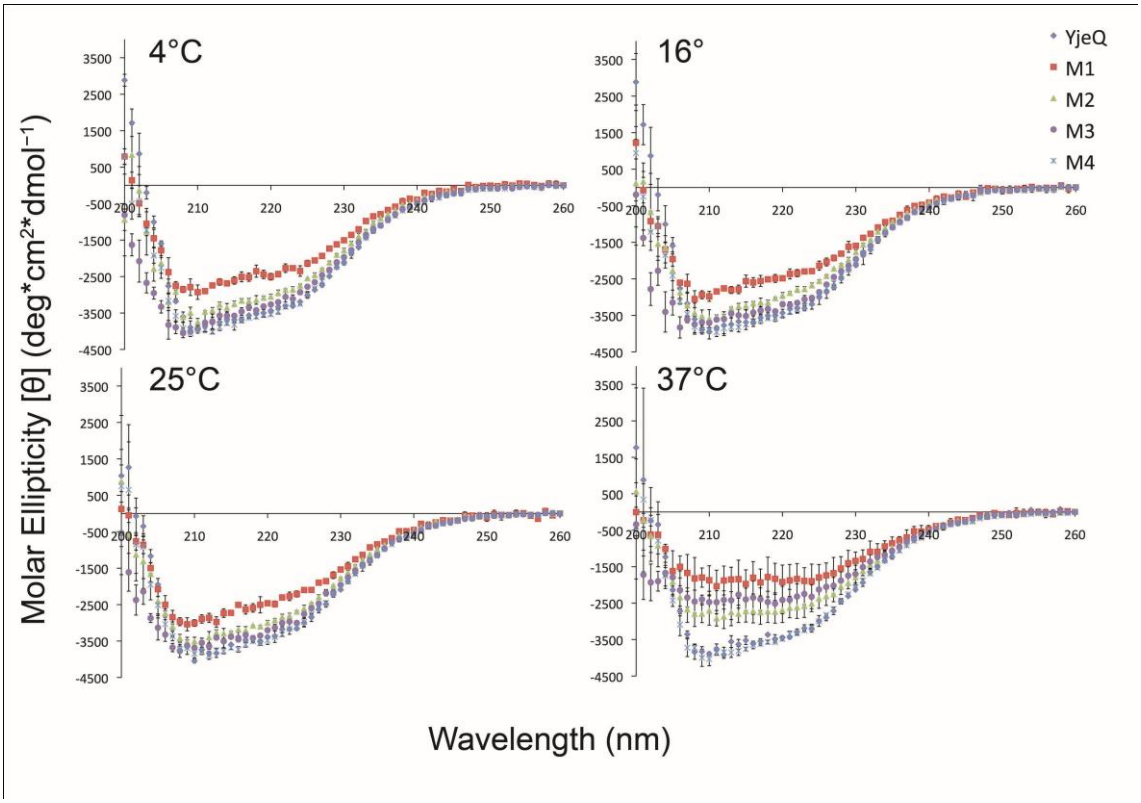

* Standard deviations are calculated from three consecutive absorbance scans

Figure 7. Circular dichroism spectra of YjeQ C-terminal variants. YjeQ, M1, M2, M3 and M4 were scanned for 15 minutes in high salt buffer (300 mM NH_4Cl) at varying temperatures of 4°C, 16°C, 25°C and 37°C. The CD spectra of each protein were scanned three consecutive times from 260 nm to 200 nm over the 15 min incubation. Molar ellipicity [θ] [deg*cm^2*dmol^{-1}] was calculated and plotted to obtain CD spectra of each protein.

Circular dichroism spectra of YjeQ showed the presence of α-helices and antiparallel β-sheets, as both secondary structures added together produced a broad negative peak from 208 nm to 222 nm (Figure 7). The YjeQ variants showed similar spectra to YjeQ, having peaks that followed a similar trend. With a decrease in presence of α-helices for the variants, peaks decreased in value. This is expected for the variants, especially for M1, which is missing the entire zinc-finger domain and has far less α-helices than the YjeQ protein (Figure 6A). The YjeQ C-terminal truncation variants (M1, M2 and M3) that had been scanned at 37°C became more unfolded compared to those at lower temperatures and scans became highly variable. This demonstrated that the precipitation observed in the previous tests (Figure 6B) was due to unstable protein folding at higher temperatures. These variants showed temperature sensitivity and future experiments with the variants were performed at temperatures no higher than 25°C.

3.2 YjeQ requires the zinc-finger domain to bind the 30S particle

The characterization of the zinc-finger domain of YjeQ for its functional significance first requires evaluating the requirement of the domain in 30S subunit binding. The OB-fold domain has already been characterized for its requirement in binding to the 30S subunit and stimulation of GTP hydrolysis of YjeQ by the 30S subunit (Daigle and Brown, 2004). The C-terminal truncation variants of YjeQ (Figure 6A) were tested for the ability to bind the mature 30S subunit (WT) and the immature 30S subunit (Δ*yjeQ*).

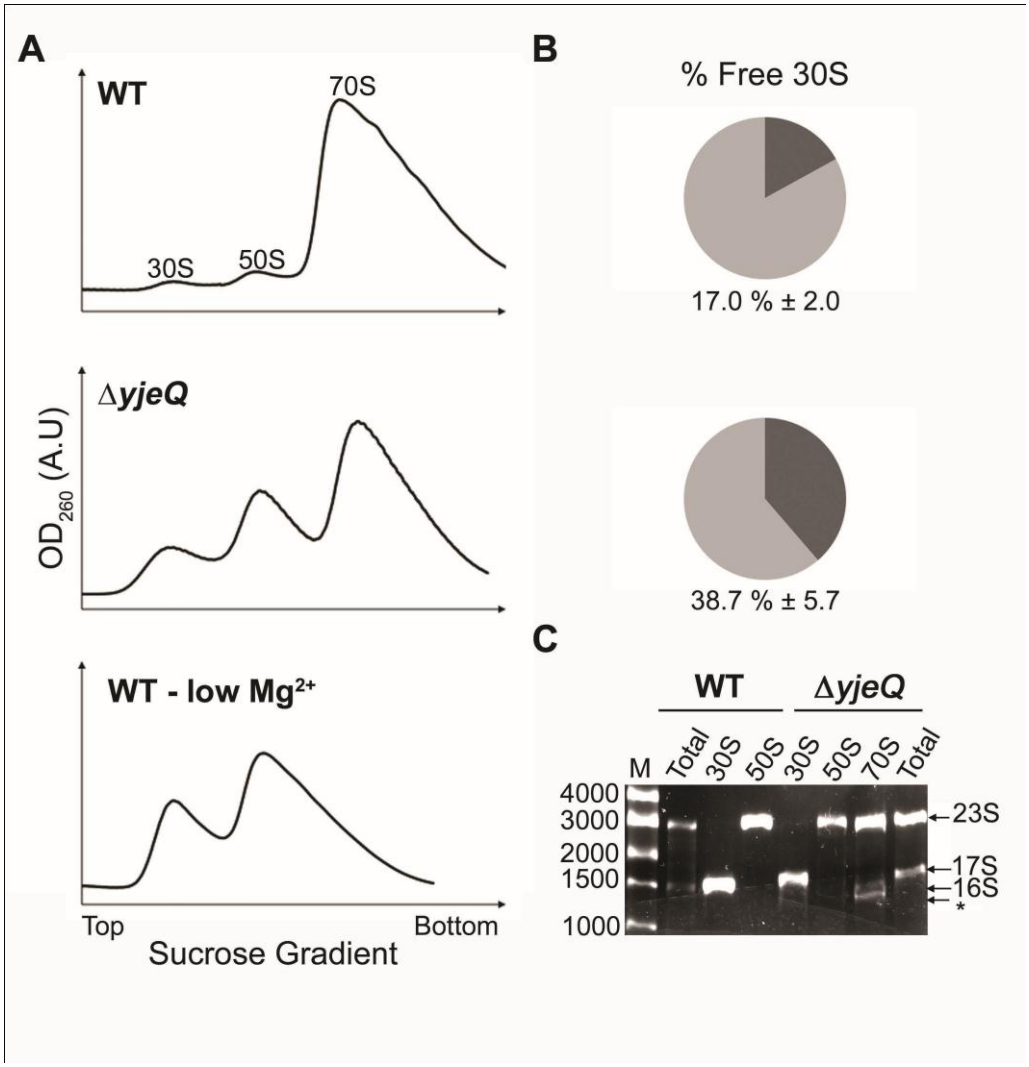

* (B) Standard deviations are calculated from two replicas of the experiment

Figure 8. Purification and characterization of the mature and immature 30S particles. (A) The ribosome profiles of the 30S particles purified from parental (WT) and Δ*yjeQ E. coli* strains. Top to bottom: WT (associated conditions-high Mg^{2+}), Δ*yjeQ* (associated conditions- high Mg^{2+}) and WT (disassociated conditions-low Mg^{2+}). (B) Percent of free 30S subunit (dark grey) over the total amount of 30S subunits in the cell (free+ 30% of 70S subunit, light grey). Each graph corresponds to ribosome profile on left. (C) The rRNA content of total rRNA (Total) in WT and *ΔyjeQ* cell cultures and in purified ribosomal subunits (30S, 50S, 70S). The marker (M) is in base pairs. The asterisk represents an unknown degradation product. Samples are run on a 0.9% synergel - 0.7% agarose gel.

Quality of 30S particles was assessed by ribosomal profiles and rRNA content. The WT *E. coli* strain yielded a profile under associating conditions (high Mg^{2+}) with a majority of 30S subunits forming mature 70S particles and only approximately 17% free 30S subunits (Figure 8A, B). In order to recover optimal amounts of mature 30S subunits, the WT strain was purified under dissociating conditions (low Mg^{2+}), which dissociate the 70S subunits (Figure 8A). Immature 30S subunits from the Δ*yjeQ E. coli* strain were obtained by purifying these subunits under associating conditions where an accumulation of approximately 39% of immature 30S subunits was observed (Figure 8A, B). This is a characteristic defect observed in the ribosome profiles of Δ*yjeQ* cells (Himeno *et al*., 2004; Jomaa *et al*., 2011a). In order to collect only immature 30S subunits, fractions of free 30S subunits were collected. The quality of the rRNA of both purified 30S particles revealed that both preparations had no contamination of 50S subunits, as there was no 23S rRNA band observed in 30S subunit preparations (Figure 8C). The mature 30S subunit was largely composed of 16S rRNA and the immature 30S subunit of 17S rRNA, which ran slightly higher than that of the 16S rRNA. A degraded product (*) beneath 16S rRNA was also observed that is occasionally found in rRNA preparations and may be a degradation product of 16S or 23S rRNA (Himeno *et al*., 2004; Jomaa *et al*., 2011a). In these studies northern blot analysis revealed it was not detected by the 16S rRNA probe and is therefore more likely a product of 23S rRNA degradation (Jomaa et al., 2011a).

YjeQ has been demonstrated to bind the mature 30S subunit tightly (Daigle and Brown, 2004; Jomaa *et al*., 2011b). Previous data suggests that YjeQ can also bind to immature 30S subunits from Δ*yjeQ* and Δ*yjeQ*Δ*rbfA* strains, but to a much lesser extent then to the mature 30S subunit (Goto *et al*., 2011). Our data suggest there is no observable difference in binding of YjeQ to the immature or mature 30S subunits (Figure 9 A, B). These results were analyzed by incubating YjeQ and YjeQ variants with 30S subunits in high salt buffer (300 mM NH_4Cl) in the presence of excess GMP-PNP at 16°C. After 15 mins the reactions were spun through a 100 kDa centrifugal device and the unbound fraction was captured in the flow-through (FT). The Bound (B) protein was resuspended with equal volume of buffer and both fractions were resolved by SDS-PAGE on 4-12% Bis-Tris gels. The YjeQ M1 variant that lacked the entire zinc-finger domain and the YjeQ M2 mutant that had only the first helix of the domain showed a reduction in binding to the mature 30S subunit compared to YjeQ (Figure 9A). The YjeQ M3 variant, which had only the c-terminal extension (CTE) truncated, did not show any observable reduction in binding to the 30S particles compared to YjeQ. However, results of the filtration assays showed that that not all M3 protein was recovered in the flow-through nor in the bound fractions. This suggested that a percentage of the M3 protein may be nonspecifically binding with the filter, despite stringent blocking of the filter with 1% BSA. To confirm that the observed binding of the M3 variant to the 30S particle was true, an additional pelleting assay was performed. In the pelleting

assay, the complex reaction is laid over a 1.1 M sucrose cushion in the same buffer used for complex formation, then subjected to ultracentrifugation. Protein that bound to the 30S subunit was found in the pellet fraction (P) and unbound protein was found in the supernatant fraction (S). The fractions were resolved by SDS-PAGE using 4-12% Bis-Tris gels (Figure 10). The results confirmed that the binding of the M3 to the 30S subunit was comparable to the binding of YjeQ to the 30S subunit using a second binding experiment.

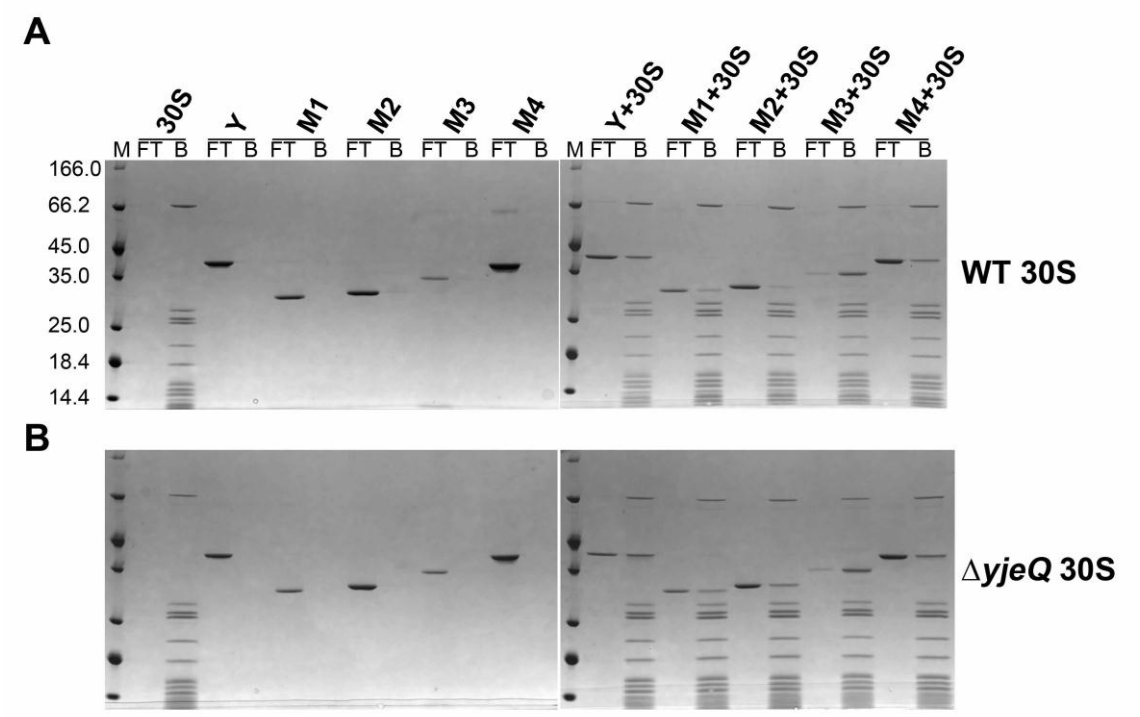

Figure 9. Binding of YjeQ C-terminal variants to the 30S particles. Ability of YjeQ (Y) and YjeQ variants (M1, M2, M3 and M4) to bind to the (A) WT and (B) Δ*yjeQ* 30S subunits was observed by filtration assays. An excess of five times protein was incubated with the 30S particles for 15 min at 16°C in the presence of GMP-PNP. Following 15 min, the reactions were subjected to ultracentrifugation with a 100 kDa cut-off filter. The unbound protein was captured in the flow-through (FT) and the bound (B) protein was retained by the filter and resuspended by equal volume of buffer. The molecular weight marker (M) is in kDa. Fractions were resolved by SDS-PAGE on 4-12% bis-tris gels.

When comparing the binding of the variants to the immature and mature 30S subunits, there appeared to be a slight increase in the amount of M1 and M2 bound to the Δ*yjeQ* 30S subunits. In the case of M3, it bound to both particles with no observable difference. This data suggests that the zinc-finger domain plays a role in tight binding of YjeQ to the mature 30S subunit but does not require the CTE for this function. It also suggests that the zinc-finger domain may not play as critical a role to tight binding to the immature 30S subunit. In this case it may depend more on the OB-fold domain to bind the immature particle.

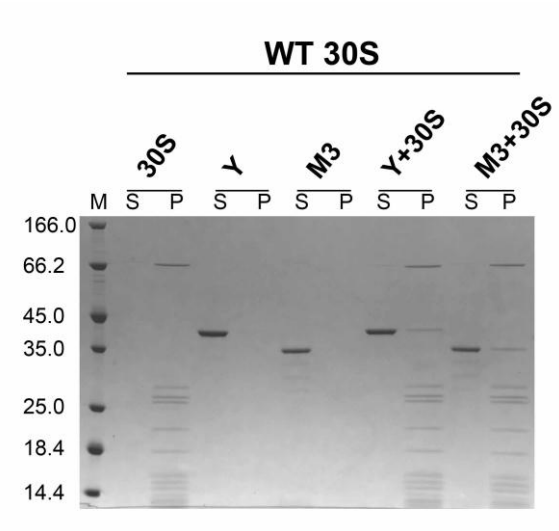

Figure 10. Pelleting Assay of M3 variant with the mature 30S subunit. An excess of five times M3 was incubated with WT 30S subunits for 15 min at 16°C. Following incubation, reactions were laid over a 1.1M sucrose cushion and subjected to ultracentrifugation. Proteins that were unbound were collected in the supernatant (S), while proteins that bound to the 30S particle were found in the pellet (P). The molecular weight (M) is in kDa. Fractions were resolved by SDS-PAGE on 4-12% bis-tris gels.

3.3 The CTE of YjeQ is necessary for 30S subunit-dependent GTPase activity

A function of YjeQ that has been observed is that there is a notable increase of the GTP hydrolysis (approximately 150-fold) that is observed in the presence of mature 30S subunits (Daigle and Brown, 2004). YjeQ itself has a slow rate of GTP hydrolysis with a k_{cat} of 9.4 hr^{-1} and a K_m for GTP of 120 μM

(Daigle *et al*., 2002). To test the GTPase activity of the YjeQ variants, a malachite green assay was used that detected the amount of free phosphate produced by reactions. The rate of GTP hydrolysis was estimated by measuring free phosphate produced by YjeQ upon incubation for one hour (Figure 11A). In this experiment, 250 µM of GTP was added to a reaction containing 100 nM of the YjeQ variant and incubated at 25°C for one hour. The reaction was quenched with malachite green reagent and absorbance was measured at 620 nm. The values were plotted against a standard curve of free phosphate in the same reaction buffer. In the case of 30S subunit-dependent reactions, there was also 100 nM of 30S particle added to the reactions. The reaction was done at 25°C and not at 30°C as done previously to measure GTP hydrolysis of YjeQ (Daigle *et al*., 2002; Daigle and Brown, 2004) in order to ensure proper folding and stability of YjeQ variants. To ensure our measurements were within the linear range of the Malachite green assay, the rate of GTP hydrolysis with half (50 nM) and double (200 nM) the concentration of 30S subunit-dependent YjeQ activity was measured. The results showed that the measurements of free phosphate obtained in our Malachite green assay experiments were within the linear range and the reactions had not reached V_{MAX} (Figure 11A).

The intrinsic GTPase activity of all C-terminal variants demonstrated that there was a low level of GTP hydrolysis observed from all variants that ranged from 1-4 pmoles/min after one hour incubation at 25°C (Figure 11B). The WT 30S subunit-dependent increase in GTP hydrolysis was not observed for any of

the C-terminal truncation variants (M1, M2, and M3) while the rate of YjeQ was increased approximately 10-fold. The fold-increase of 30S subunit-dependent GTP hydrolysis of the protein over protein alone was measured by subtracting the background level of GTP hydrolysis by the 30S particle. This may be lower than the fold-increase observed by Daigle *et al.*, due to lower temperature conditions and variations within protein and ribosome purifications. The immature (Δ*yjeQ*) 30S subunit-dependent reactions showed a slight increase in GTP hydrolysis of YjeQ of approximately 3-fold, but again no increase was observed by C-terminal truncation variants. This supports previous studies that show the stimulation of GTPase activity of YjeQ by the immature 30S subunit is minimal in comparison to the mature 30S subunit (Himeno *et al*., 2004).

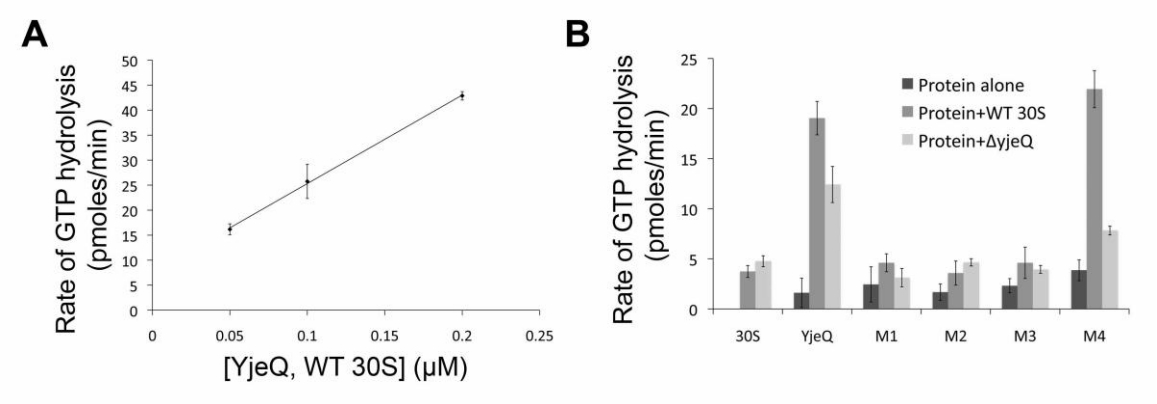

* Standard deviations are calculated from three replicas of the experiment

Figure 11. GTPase activity of YjeQ C-terminal variants. (A) Graph showing the rate of GTP hydrolysis is within the range of initial rate. The GTP hydrolysis of YjeQ at different concentrations (50 nM, 100 nM and 200 nM) with stoichiometric amounts of 30S subunit was measured after 1 hr incubation at 25°C with 250 μM GTP in high salt buffer (300 mM NH_4Cl). (B) GTP hydrolysis of YjeQ variants compared to 30S subunit-dependent GTP hydrolysis measured with enzyme and 30S subunit at a concentration of 100 nM.

The YjeQ variants (M1 and M2) did not show an increased level in 30S subunit-dependent GTPase activity, likely because both proteins cannot efficiently bind the mature 30S particle (Figure 9A). However, M3 was able to bind the 30S subunit but showed no increase in 30S subunit-dependent GTPase activity. These results suggested that while the zinc-finger domain may be required for binding, the C-terminal extension of the domain is necessary for stimulation of GTP hydrolysis by the 30S subunit. The CTE is oriented in a way that would directly interact with helix 44 of the mature 30S subunit when YjeQ is bound (Jomaa *et al*., 2011b), suggesting that contact of the two helices may provide the signal for GTP hydrolysis and removal of YjeQ.

3.4 YjeQ is unable to remove RbfA from the 30S subunit without the CTE

Genetic and biochemical studies have shown that there is a direct link between the removal of RbfA from the 30S subunit and binding of YjeQ to the 30S subunit (Goto *et al*., 2011). Mutants of RbfA that decreased the ability of the protein to bind to the 30S subunit were able to suppress growth defects of the Δ*yjeQ* strain. This suggested that the role of YjeQ was to displace RbfA and YjeQ was not required for growth when RbfA did not tightly bind the 30S subunit. These genetic studies were supported by biochemical experiments that showed YjeQ was able to displace RbfA on the mature 30S subunit, but not the immature 30S subunit when bound to GTP or GDPNP. What is not clearly understood by these studies is the mechanism behind the removal of RbfA by YjeQ and the functional significance of this interplay to the maturation of the 30S subunit. In

this case, the YjeQ M3 variant can be used as a tool to assess the removal of RbfA from the 30S subunit by a variant of YjeQ that binds binds the 30S subunit but is not stimulated to hydrolyze GTP. This variant can be used to provide further understanding about the role of the YjeQ zinc-finger and the interplay of YjeQ with RbfA in the maturation of the 30S subunit.

The interplay of YjeQ and RbfA was assessed on the WT and Δ*yjeQ* 30S subunits that were characterized in Figure 8. RbfA was found to minimally bind the mature 30S subunit and required incubation in a low salt buffer (60 mM NH_4Cl) to observe optimal binding (Figure 12A). In the reaction where WT 30S subunit was incubated with RbfA then YjeQ, RbfA no longer bound to the 30S subunit (Figure 12B). This suggested verified that YjeQ was able to cause removal of RbfA from the mature 30S subunit as observed previously (Goto *et al*., 2011). However, it should be noted that in our findings, binding of RbfA to the mature 30S subunit was minimal and required a decrease in salt to be observed by filtration assay. To assess the interplay of RbfA and YjeQ during maturation of the 30S subunit, it is more informative to assess binding of these two proteins to the immature 30S subunit. As shown previously, YjeQ was able to bind both the WT and Δ*yjeQ* 30S subunits in high salt buffer (300 mM NH_4Cl) based on filtration assays (Figure 9A). In high salt buffer, RbfA was not shown to bind the WT 30S subunit or cause an observable difference in binding of YjeQ to the 30S subunit (Figure 12C). However, RbfA was able to bind the Δ*yjeQ* 30S subunit and remain bound in the presence of YjeQ. This demonstrates that RbfA binds

tightly to the immature 30S subunit under high salt conditions and could not be removed by YjeQ as it was on the mature 30S subunit.

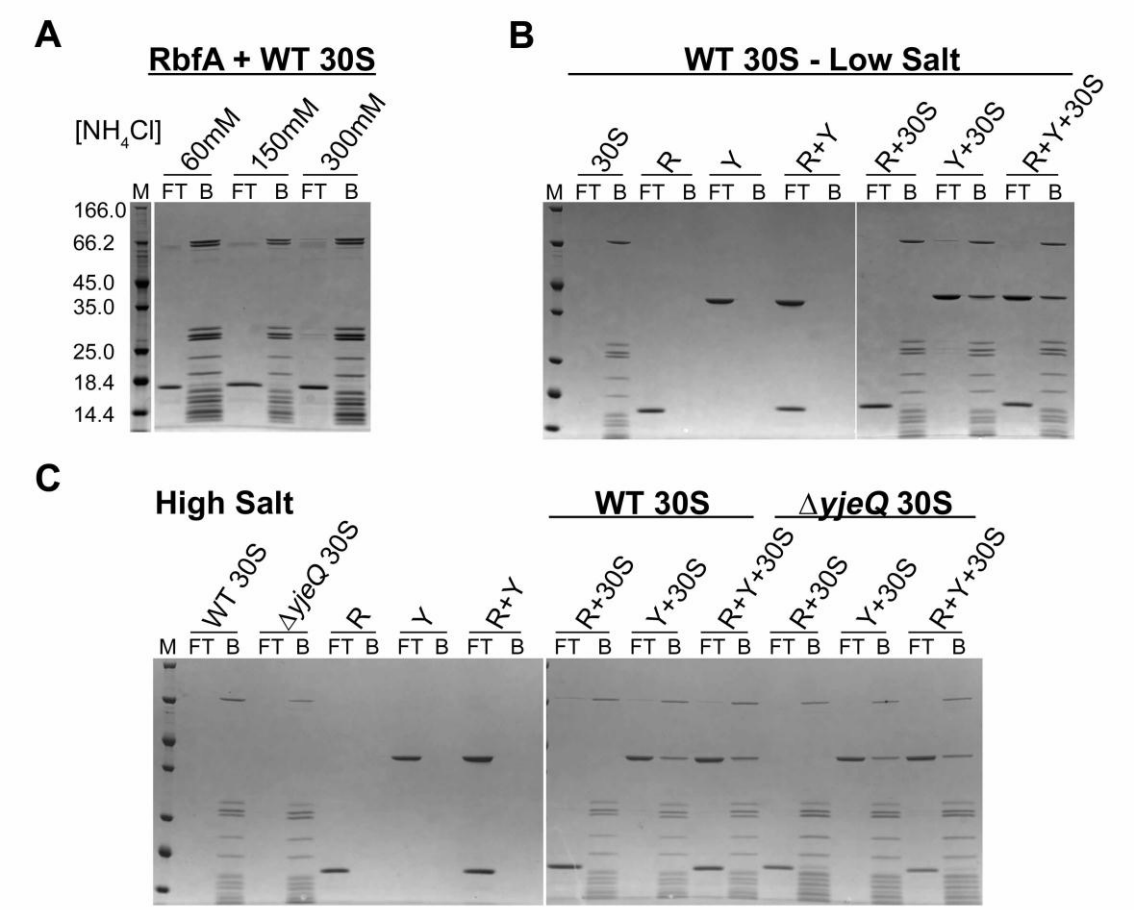

Figure 12. Interplay of YjeQ and RbfA on the 30S particle. Binding experiments were performed by incubating RbfA with 30S particle in low or high salt buffer for 15 minutes. Reactions were incubated for an additional 15 mins upon addition of YjeQ and GMPPNP. Flow-through (FT) containing unbound protein and bound (B) protein retained on the filter were separated by ultracentrifugation through a 100-kDa cut-off centrifugal device. Fractions were resolved by SDS-PAGE on 4-12% Bis-tris gels. The molecular weight marker (M) is in kDa. (A) RbfA was incubated with WT 30S subunit in varying salt buffers to determine optimal binding conditions. (B) YjeQ (Y) was added to the RbfA (R) complex with WT 30S subunit under low salt. (C) YjeQ and RbfA interplay on the WT and Δ*yjeQ* 30S subunits under high salt.

The location of RbfA is within the neck of the 30S subunit behind h44, causing displacement of densities that appear to be h44 and h45 towards the interface (Datta *et al*., 2007). It is possible that YjeQ causes removal of RbfA from the mature 30S subunit via mechanical displacement of h44, which it too has been shown to displace when bound (Figure 4A) (Jomaa et al., 2011b). If the conformational shift of h44 observed in the complex of YjeQ and the mature 30S subunit is induced by the zinc-finger domain, then there may be a link between the function of the zinc-finger domain and RbfA. To test the function of this domain in the interplay between RbfA and YjeQ, it would be beneficial to assess the interplay between RbfA and M3. The YjeQ M3 variant was chosen because it was able to effectively bind both the mature and immature 30S subunits (Figure 9A,B) but its GTPase activity was not stimulated by the 30S subunit (Figure 11B) and it therefore does not function as wild-type YjeQ.

A filtration assay was performed to detect removal of RbfA from the WT 30S subunit by M3 compared to YjeQ. Unlike the filtration assays done previously for RbfA with YjeQ, these reactions were incubated at 25°C, in order to maintain the solubility and folding of M3. At 25°C, the removal of RbfA on the 30S subunit by YjeQ was minimal but observed (Figure 13A). When M3 was incubated with the RbfA:30S subunit complex, an enhanced binding of RbfA to the 30S subunit was observed instead of removal of the protein. To ensure the result was not due to RbfA getting stuck on the filter in the presence of both 30S subunits and M3, the binding experiment was repeated with a pelleting assay.

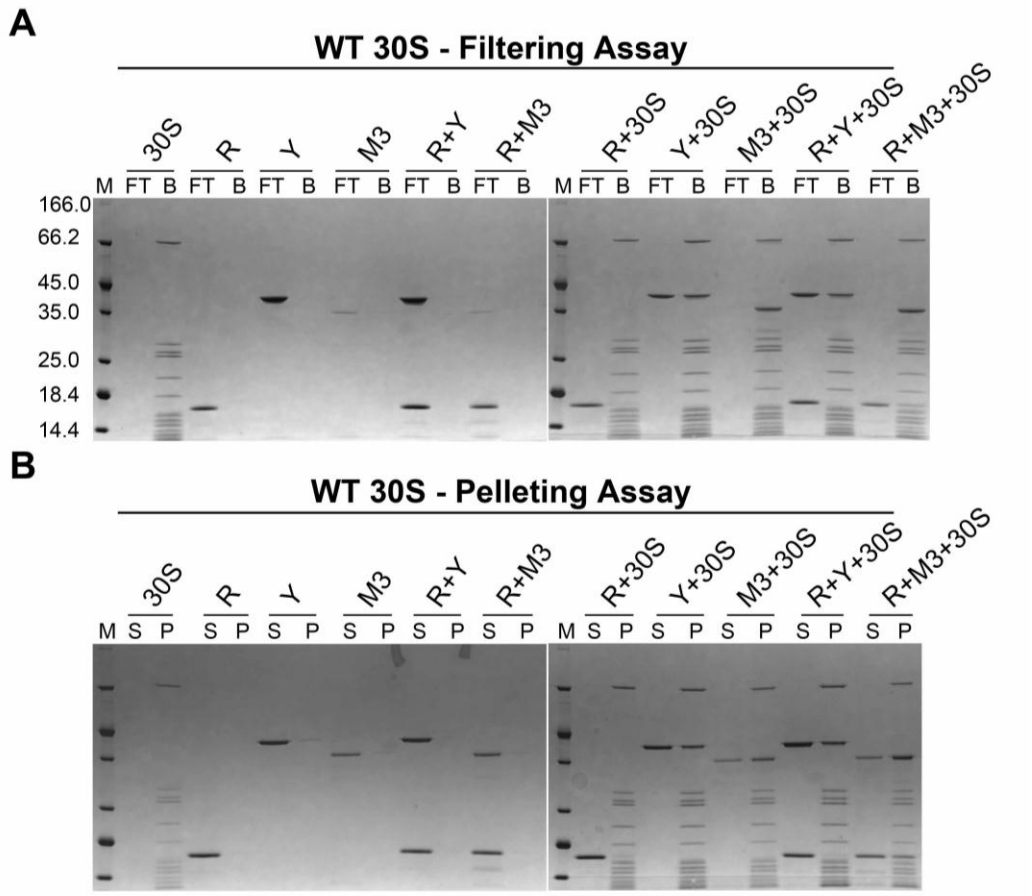

Figure 13. Interplay of the M3 variant of YjeQ with RbfA on the mature 30S subunit. (A) Filtration assay to test binding of RbfA (R) in the presence of YjeQ (Y) or M3 with GMP-PNP on the maturation (WT) 30S subunit following incubation at 25°C for 15 min. Proteins were added in five times excess of 30S particles. (B) Pelleting assay of identical reactions used in (A). The molecular weight marker (M) is in kDa. Fractions were resolved by SDS-PAGE using 4-12% Bis-tris gels.

This eliminated with use of the filter and was a more stringent assessment to test the interplay of RbfA with M3. The pelleting assay supported findings from the filtration assay (Figure 13B). These results suggest that the zinc-finger domain, specifically the CTE of the domain, has a direct effect on the binding of RbfA to the 30S subunit.

3.5 The M3 variant is unable to complement the function of YjeQ *in vivo*

The *in vitro* studies performed with the YjeQ C-terminal truncation variants demonstrated that the CTE of the YjeQ zinc-finger may be a crucial element for the function of YjeQ in ribosome biogenesis. The M3 variant that was truncated at the CTE showed an ability to bind the 30S subunit (Figure 10) but was not stimulated to hydrolyze GTP (Figure 11B) or remove RbfA (Figure 13). To test whether this helical extension is necessary for the function of YjeQ *in vivo* the growth curves, ribosomal RNA and ribosome profiles were analyzed.

Table 2. Doubling-time and growth rates of the *E. coli* strains in LB liquid media.

***E. coli* strains**	**Double time (DT) (hr)**	**Growth rate k=ln2/DT (hr^{-1})**
Parental (WT)	1.57±0.03	0.44±0.01
Δ*yjeQ*	4.86±0.16	0.14±0.01
ΔyjeQ+p-*empty* (1 µM IPTG)	4.92±0.08	0.14±0.01
ΔyjeQ+p-*empty* (100 µM IPTG)	5.25±0.05	0.13±0.01
ΔyjeQ+p-*yjeQ* (1 µM IPTG)	3.33±0.05	0.21±0.01
ΔyjeQ+p-*yjeQ* (100 µM IPTG)	5.57±0.22	0.12±0.01
ΔyjeQ+p-$m3^A$ (1 µM IPTG)	7.25±0.08	0.10±0.01
ΔyjeQ+p-$m3^A$ (100 µM IPTG)	3.75±0.05	0.18±0.01

***** Standard deviations were calculated from three replicas of the experiment.

The *E. coli* strains were grown at 25°C and allowed to grow up to 47 hours. Optical density (OD) of cell cultures grown in a 96-well plate was measured at 600 nm every 10 minutes. Every tenth absorbance value was plotted on a growth curve (Figure 14A). Strains that were complimented with plasmids were induced with 1 or 100 µM of IPTG at time zero.

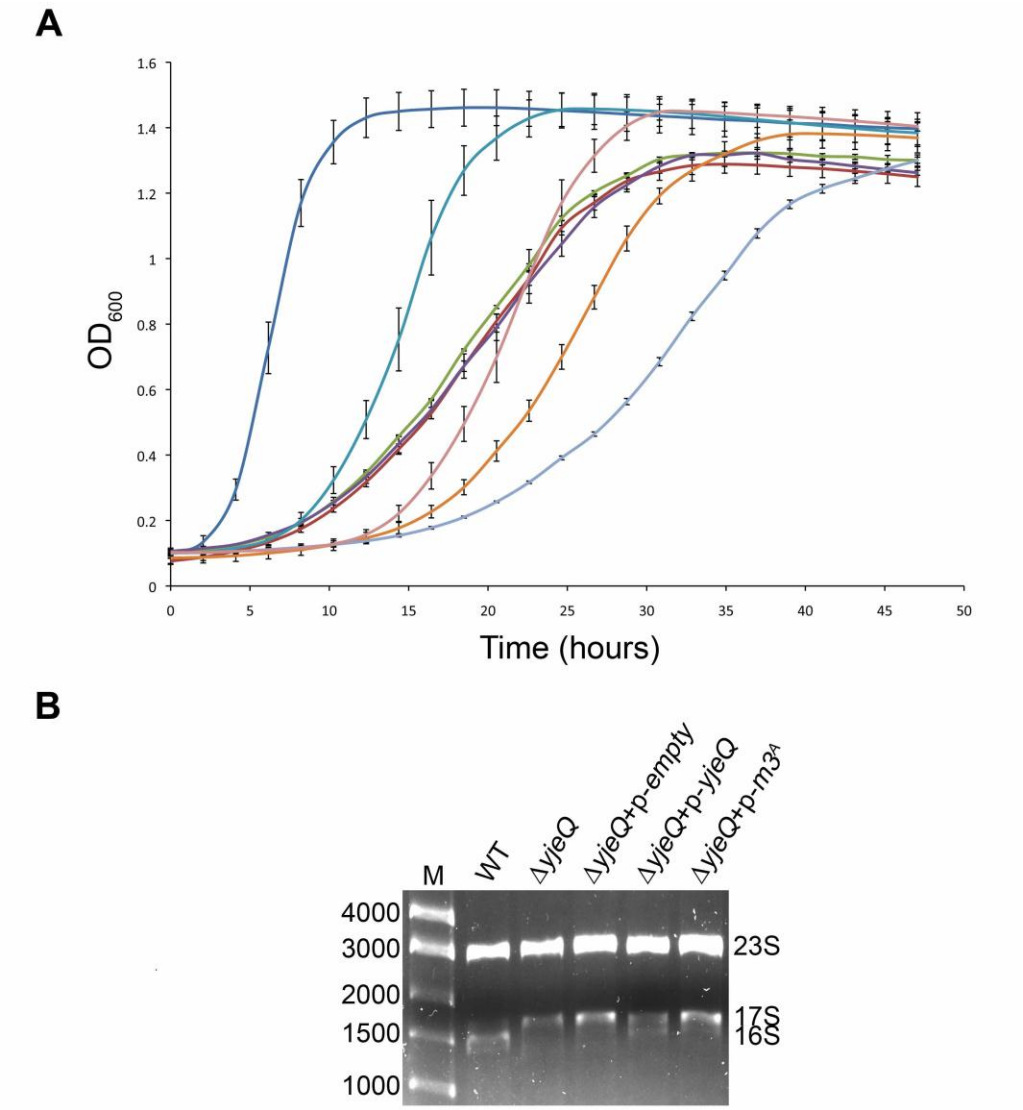

Figure 14. Growth and rRNA analysis of *E. coli* strains. *E. coli* Δ*yjeQ* strains were complemented with p-*empty*, p-*yjeQ* or p-*m3*^{A} at time zero and cells were grown at 25°C for 47 hrs. (A) Growth curves represent absorbance at 600 nm of cell cultures grown in three replicas in a 96-well plate. (B) Total rRNA of cell cultures were analyzed when cultures reached mid-log phase represented by an OD 0.2. Total rRNA was extracted and resolved by 0.9% synergel - 0.7% agarose gel. The marker (M) is in base pairs. The asterisk represents an unknown degradation product.

Cells were grown at 25°C to ensure proper folding and solubility of M3. Doubling-time and growth rates for all *E. coli* strains that were assessed in Figure 14A are listed in Table 2.

Characterization of the Δ*yjeQ* strain revealed that the strain grew at a rate of 0.14 hr^{-1}, approximately three times slower than WT, which grew at 0.44 hr^{-1}. This is slower than the Δ*yjeQ* strain grown at 37°C (Himeno *et al*., 2004). However, this is not unusual for ribosomal assembly factors since absence of these factors cause cells to have a cold-sensitive phenotype (Shajani *et al*., 2011). When complimented by a low induction of YjeQ (1 µM IPTG), the Δ*yjeQ* strain grew approximately 1.5 times faster than Δ*yjeQ* with empty plasmid. However, when complimented by higher induction of YjeQ (100 µM IPTG) the strain grew at a rate of 0.12 hr^{-1}, slightly slower than the rate of Δ*yjeQ*. This is likely a toxic effect caused by an excess of YjeQ in the cells, which can cause 70S subunits to disassemble (Himeno *et al*., 2004). When the YjeQ M3 variant was complimented by a low induction, the results revealed that the cells grew at a rate of 0.10 hr^{-1}, far slower than that of WT and Δ*yjeQ* cells. The rate was 4.5 times slower than WT cells and 1.5 times slower than Δ*yjeQ* cells. This demonstrated that the M3 variant *in vivo* was not able to compliment the slow-growth phenotype of Δ*yjeQ* cells. It was noted that when M3 was complimented at a higher induction, the growth rate increased in comparison to a lower induction by about 1.8 times. This was opposite to the findings for when the induction of YjeQ was increased, which caused the rate of cells to slow down due

to toxicity. It is possible that in this case high amounts of M3, which demonstrated unstable folding at higher temperatures and lower salt concentrations, may be aggregating and moved out of the cell by inclusion bodies. Due to the fact that wild-type YjeQ protein expressed at this concentration is already toxic, the mutant protein may be causing some additional stress on the cells that is unclear. In the following studies of the rRNA content and ribosomal profiles of the *E. coli* strains, only the complementation experiments induced with 1 µM IPTG were studied to avoid possible findings resulting from protein toxicity.

The total rRNA of the *E. coli* strains was extracted by cell cultures from an OD_{600} of 0.2 to ensure cells were at mid-log phase. Analysis of rRNA revealed that total rRNA from WT cells was a majority of 16S rRNA, where a small amount of 17S and a degraded product (*) beneath 16S rRNA was also observed (Figure 14B). The rRNA from Δ*yjeQ* mainly consisted of 17S rRNA. When complimented with p-*empty*, p-*yjeQ* and p-$M3^A$, only the expression of YjeQ was able to produce more 16S rRNA containing 30S particles, whereas the expression of M3 had no effect on processing of 17S rRNA. The YjeQ M3 variant was unable to recover maturation of the 17S rRNA *in vivo*.

The removal of ribosome assembly factors causes an accumulation of immature 30S and 50S subunits and a decrease in 70S subunits. In the case of WT cells, the ribosome profiles revealed minimal peaks of free 30S and 50S subunits but a large peak for the 70S subunits (Figure 15A).

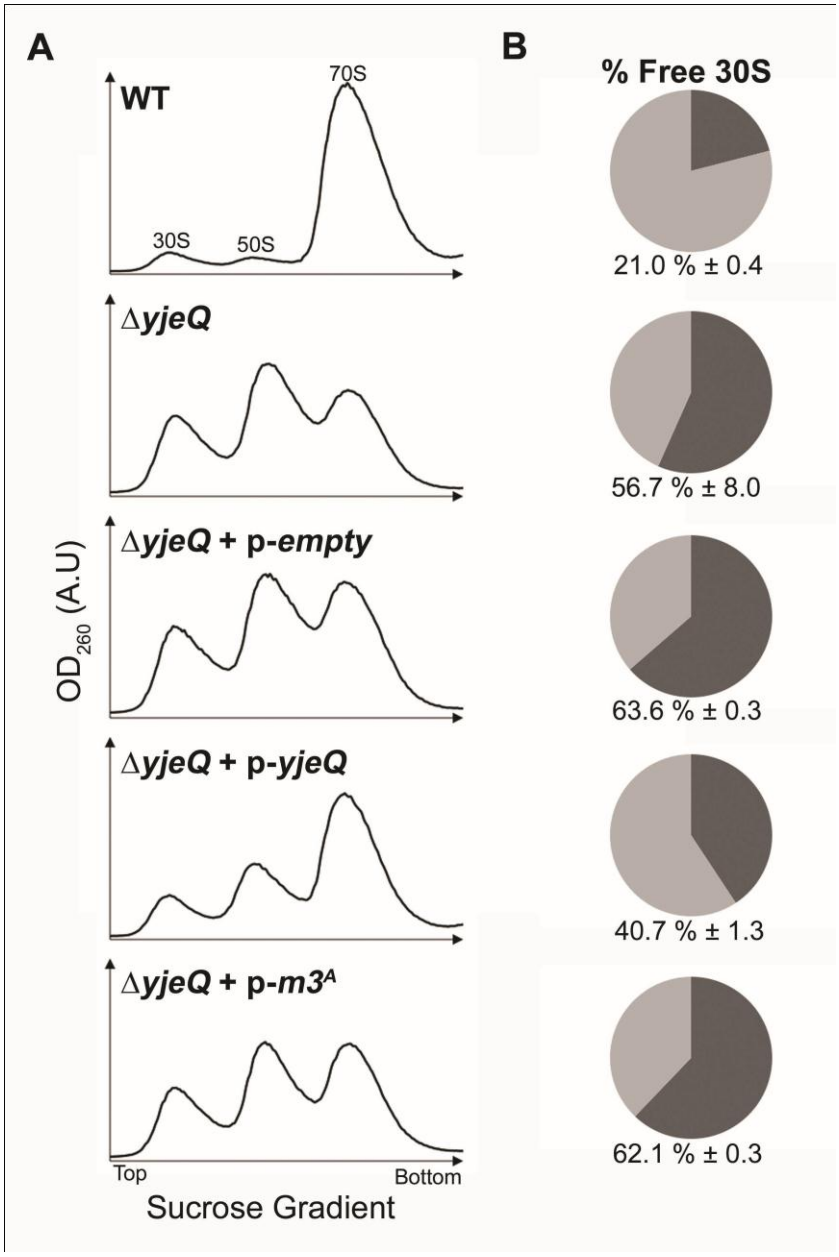

Figure 15. Ribosome profiles of *E. coli* strains. (A) The ribosome profiles of the WT strain and the Δ*yjeQ* strain complimented with p-*empty*, p-*yjeQ* and p-$M3^A$ were analyzed by 10-30% sucrose gradient ultracentrifugation. Cells were grown at 25°C to an OD_{600} of 0.2. Absorbance of ribosome peaks were measured at 260 nm. (B) Percent of free 30S subunit (dark grey) over the total amount of 30S subunits in the cell (free+ 30% of 70S subunit, light grey). Each graph corresponds to ribosome profile on left.

Less than 1/5 of the total 30S subunit content of the cells was free while a majority of the 30S subunits formed functional 70S particles (Figure 15B). The Δ*yjeQ* strain contained a clear accumulation of 30S and 50S subunits with a decreased peak of 70S subunits (Figure 15A). More than half the 30S subunits in this strain were free and not able to bind to the 50S subunits to form functional 70S particles (Figure 15B). The results of the *in vivo* complementation assays of p-*empty*, p-*yjeQ* and p-$M3^A$ revealed that only the p-*yjeQ* plasmid is able to rescue the ribosome profile of the Δ*yjeQ* strain. The amount of free 30S subunits moves to less than 2/5 of the total 30S subunit content in the cell. However, expression of M3 was unable to neither decrease the percentage of free 30S subunits in the cell nor increase it. This suggests that M3 is not able to function as wild type YjeQ *in vivo*. Expression of M3 *in vivo* leads to a slower growth rate of Δ*yjeQ* cells and no observable increase of 16S rRNA or decrease in accumulation of free 30S subunits.

3.6 The zinc-finger domain of YjeQ is unlikely to interact with the head of 30S Subunit

Previous studies that have resolved the structure of the complex of YjeQ with the mature 30S subunit have revealed that there is a second possible orientation in which YjeQ binds the particle (Guo *et al*., 2011). This structure revealed that YjeQ bound in an orientation in which the zinc-finger domain interacted with the head of the 30S subunit and the OB-fold domain interacted with h44 (Figure 16). Upon close inspection of the interaction of the zinc-finger

domain of YjeQ with the head of the 30S subunit, it appears that the key interactions would occur through a small patch of positive charges in the zinc-binding motif. This patch (blue) is identified by the arrows in the zoomed-in left and right bottom panels of Figure 16. These positive charges can specifically be accounted for by the residues of lysine 298 and arginine 300. If these charges were neutral than the largely negative zinc-finger domain should likely be unable to bind the head domain, since a majority of the domain is not in contact with any of the rRNA or r-proteins of the 30S subunit in this structure. To assess whether these positive residues were required to bind the 30S subunit, a point mutant of YjeQ was created by mutagenesis. The YjeQ M4 variant contained a point mutation of L298A and R300A, where both positively charged residues were mutated to neutral alanine residues (Figure 6A). Unlike the C-terminal truncation variants of YjeQ, M4 did not demonstrate any temperature insolubility (Figure 6B) or folding instability (Figure 7). However assays done with M4 were carried out in parallel to the C-terminal truncation variants and were therefore subjected to the same experimental conditions.

The YjeQ M4 variant showed no effect on binding to the WT or Δ*yjeQ* 30S subunits and its binding was comparable with wild-type YjeQ to the 30S particles (Figure 9A,B). The YjeQ M4 variant was stimulated to hydrolyze GTP more than five-fold by the mature 30S subunit and minimally by the immature 30S subunit (Figure 11B). These experiments showed that M4 behaved similarly to wild type

YjeQ and was unaffected by the loss of two key positive charges that would be required for the YjeQ zinc-finger domain to bind the head of the 30S subunit.

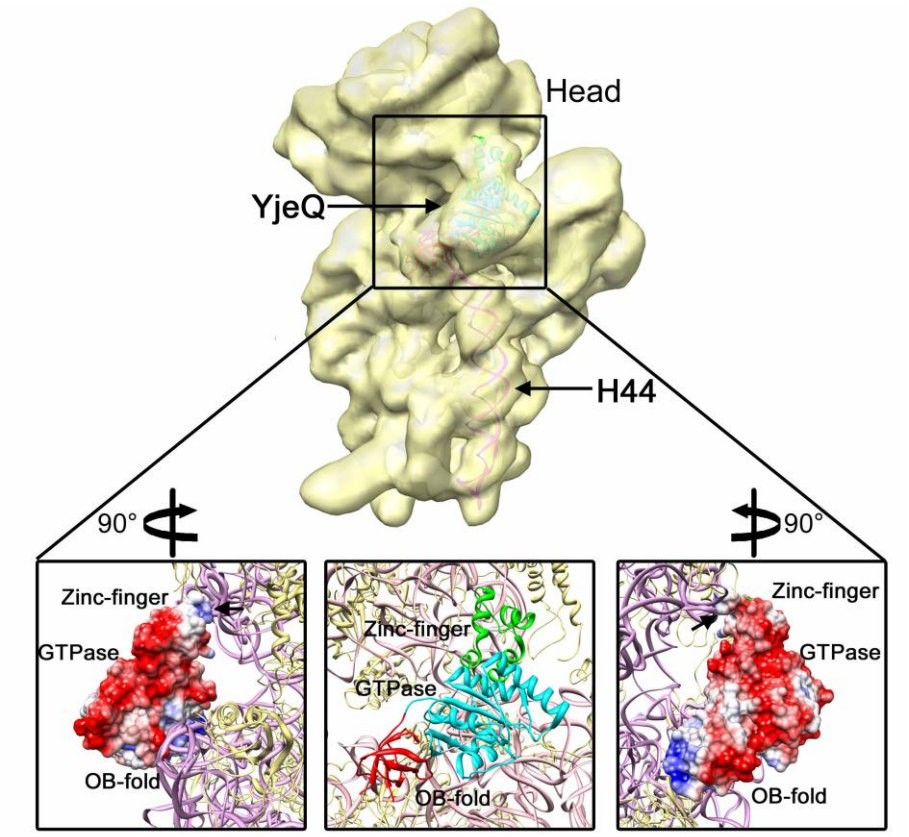

Figure 16. Orientation of YjeQ bound to the 30S subunit solved by Gao lab. The cryo-EM structure of YjeQ bound to the WT 30S subunit (EMDB 1884 fitted with PDB 2YKR). Beneath is the zoom in views of YjeQ bound to the 30S subunit, the 16S rRNA (purple) and the r-proteins (beige) are shown around the binding site of YjeQ. The left and right images show the electrostatic potential map of YjeQ. Zones are negatively charged (red), positively charged (blue) and uncharged (white). The positive patch of YjeQ in the zinc-finger domain that interacts with the head domain of the 30S subunit is identified by arrows.

However, if YjeQ binds in the orientation in which the zinc-finger domain interacts with h44 (Figure 4A) (Jomaa *et al*., 2011b), than these two residues are pointing outwards from the interface and should have minimal effect on binding or

hydrolysis of YjeQ by the 30S subunit. Therefore there is little evidence to support the binding of YjeQ with the orientation in which the zinc-finger domain interacts with the head of the 30S subunit. This will remain unclear until a higher resolution structure of YjeQ in complex with the 30S subunit is solved.

4. DISCUSSION

The YjeQ protein has been identified as a GTPase involved in the assembly of the 30S subunit in bacteria (Daigle *et al*., 2002; Himeno *et al*., 2004). Deletion of YjeQ results in a slow-growth phenotype of cells and accumulation of immature 30S subunits with unprocessed 17S rRNA (Himeno *et al*., 2004; Jomaa *et al*., 2011a). This immature 30S subunit has a distorted decoding centre in the same region that YjeQ binds on the mature 30S subunit (Guo *et al*., 2011; Jomaa *et al*., 2011a; Jomaa *et al*., 2011b; Kimura *et al*., 2008). Recent structural studies of immature 30S subunits accumulated in the absence of other assembly factors such as RimM (Clatterbuck Soper *et al*., 2013; Guo *et al*., 2013; Leong *et al*., 2013), KsgA (Boehringer *et al*., 2012), RbfA (Clatterbuck Soper *et al*., 2013) and a double knock-out of YjeQ and RbfA (Yang *et al*., 2014) have also found that the decoding centre is not formed in these intermediates. Interestingly, new insights into the structural intermediates of the 50S subunit accumulated in the absence of assembly factor RbgA (YlqF) have revealed that the peptidyl-transferase centre, which is the functional core of the 50S subunit, is also not formed (Jomaa *et al*., 2014; Li *et al*., 2013). These studies have all revealed that ribosome assembly factors play a key role in final formation of the functional core of the 30S and 50S subunits.

Based on the structure of YjeQ bound to the 30S subunit, previously solved by our lab using cryo-EM (Jomaa *et al*., 2011b), we hypothesized that the distortion of the decoding centre could be mediated through interaction of the

zinc-finger domain of YjeQ with h44. Using YjeQ C-terminal variants with deletions in the zinc-finger domain, we found that the zinc-finger domain is required for binding of YjeQ to the 30S subunit and stimulation of GTPase activity. We also found that the zinc-finger domain of YjeQ is required for removal of the assembly factor, RbfA, from the 30S subunit. These results suggests that following assembly factor-mediated formation of the decoding centre, YjeQ and other assembly factors are signaled to release from the mature 30S subunit. YjeQ likely acts as a checkpoint protein that detects final conformation of the decoding centre while other assembly factors, such as RbfA, act as chaperones for rRNA folding.

4.1. The role of the zinc-finger domain of YjeQ in 30S subunit biogenesis

Truncation of the C-terminal zinc-finger domain of YjeQ yielded variants that were unable to bind the mature 30S subunit tightly (Figure 9A). However, in the absence of only the C-terminal extension (CTE) of YjeQ in the M3 variant, the protein was still able to bind the 30S subunit but showed no stimulation of GTPase activity. The OB-fold domain of YjeQ was previously shown to be required for binding to the 30S subunit and without efficient binding it was not stimulated to hydrolyze GTP (Daigle and Brown, 2004). Results of the C-terminal variants suggest the domain has an additional function, aside from binding, which allows it to induce activation of the GTPase domain.

Analysis of other circularly permutated GTPases involved in ribosome assembly suggests that a potential function of the C-terminal domain is linked to

stimulation of GTPase activity. These assembly factors, RbgA (YlqF), YawG and YqeH, all have C-terminal domains downstream of the GTPase domain just as YjeQ does (Anand *et al*., 2006). The C-terminal domains are characteristic of RNA-binding domains but the role of the domains remain unclear (Elias and Novotny, 2008; Kim do *et al*., 2008; Sudhamsu *et al*., 2008). What is unique about these circularly permuted GTPase domains is the arrangement of the sequence motifs (Anand *et al*., 2006). Instead of having an order of G1-G5 motifs, the order is G4-G5-G1-G2-G3, but the tertiary structure of the domain remains unchanged. This results in the switch I and switch II regions that coordinate the binding of Mg^{2+} and the γ-phosphate of GTP, which are typically centrally located (Sprang, 1997), to be located further downstream of the domain (Anand *et al*., 2006). As a consequence, the regions just outside these domains can induce GTP hydrolysis when undergoing large conformational changes or can undergo large conformational changes as a result of GTP hydrolysis. The switch II region of the YjeQ GTPase domain is linked via a connecting loop directly to the C-terminal domain and is therefore likely directly affected by the circular permutation (Shin *et al*., 2004). The results revealed that without the CTE, the GTPase activity of YjeQ was not stimulated and that there is a link between 30S subunit-dependent GTPase activity and the C-terminal domain. This suggests that a conformational change of the CTE propagates a mechanical effect upstream to the GTPase domain, resulting in hydrolysis of GTP and removal of YjeQ from the 30S subunit. Given the location of h44 in relation to the

zinc-finger domain, we conclude that this stimulation is possibly occurring following formation of the decoding centre.

Further evidence that a conformational change of h44 induces hydrolysis of GTP by YjeQ via the zinc-finger domain is in the structure of the immature 30S subunit. The structure reveals that YjeQ has an unformed decoding centre that would likely not interact with the zinc-finger domain of YjeQ until it is stabilized in a mature conformation (Jomaa *et al*., 2011a). Therefore there would be minimal contact between h44 and the zinc-finger domain of YjeQ. This would support the findings that YjeQ did not demonstrate as high of a stimulation of GTPase activity when bound to the immature 30S subunit from Δ*yjeQ* cells as it did when bound to the mature 30S subunit (Figure 9B). These results were also observed by previous measures of GTPase activity of YjeQ in the presence of immature 30S subunits accumulated from Δ*yjeQ*Δ*rbfA* cells (Goto *et al*., 2011).

These conclusions are based on the assumption that h44 interacts with the zinc-finger domain of YjeQ from a previously solved cryo-EM structure of YjeQ in complex with the mature 30S subunit (Jomaa *et al*., 2011b). However, it is important to note that there was an additional complex of YjeQ bound to the 30S subunit that was solved by Guo *et al*. This complex revealed that YjeQ binds in an orientation in which the OB-fold domain interacts with h44 and the zinc-finger domain interacts with the head of the 30S subunit (Figure 16) (Guo *et al*., 2011). This orientation of YjeQ binding was incompatible with our current findings. A C-terminal double-point mutant of YjeQ, M4, revealed that mutations

L298A and R300A yielded no negative effect on the function of YjeQ binding to the 30S subunit (Figure 9) or 30S subunit-dependent GTPase activity (Figure 11B). In the orientation in which YjeQ binds the head of the 30S subunit via the zinc-finger domain, these two positive residues of YjeQ are the main points of contact with the 30S subunit. The remainder of the zinc-finger domain has minimal contact with the 30S subunit and is located between the head and the platform of the 30S subunit. This orientation would also not provide a model for the role of the CTE of YjeQ in 30S subunit maturation. Interaction of the CTE with both the immature and mature 30S subunits would be largely unchanged since the head domain does not undergo dramatic conformational changes such as that of h44. Therefore, our results conclude that the role of the YjeQ zinc-finger domain is to bind the 30S subunit and be stimulated to hydrolyze GTP upon interaction with h44, once it is in a mature conformation.

4.2 The zinc-finger domain of YjeQ plays a critical role to its function *in vivo*

Results from the function of the C-terminal extension variant *in vivo* revealed that it is unable to complement the phenotype of YjeQ. Growth curves showed that Δ*yjeQ* cells complimented with a plasmid encoding for M3 grew slower than Δ*yjeQ* cells (Figure 14A, Table 2). Complementation of M3 in Δ*yjeQ* cells yielded no decrease in 17S rRNA (Figure 14B) or changes in the Δ*yjeQ* ribosome profile (Figure 15). This data showed that the CTE of YjeQ was required for the function of YjeQ *in vivo*.

What should be noted is that although the rRNA and ribosome profiles of Δ*yjeQ* cells complemented with M3 were unchanged, the growth rate was slower. This could be due to a portion of the M3 variant, which showed some instability in secondary folding (Figure 7), potentially aggregating and requiring additional cellular resources to remove mis-folded protein into inclusion bodies (Sabate *et al*., 2010). This would slow down the growth of cells but would not influence the ribosome profile of the immature 30S subunits that have already accumulated. What is interesting to note is that when a large amount of the M3 variant was expressed with 100 µM IPTG, the growth rate was faster than that of Δ*yjeQ* cells (Table 2). This finding would suggest that with large amounts of M3 variant produced, the Δ*yjeQ* cells are able to overcome the slow-growth phenotype. This finding was unexpected, but suggested that cells may take an alternative pathway to ribosome biogenesis independent of YjeQ in the presence of stress caused by over-expression of toxic protein. This may be a similar mechanism to that taken by Δ*yjeQ* cells that confer resistance to high salt stress (Hase *et al*., 2009). Although the cause of this finding is unclear, these results reveal that the CTE of YjeQ is essential to the function of the protein with assisting ribosome assembly *in vivo*.

Recent mutational analysis of the circularly permutated GTPase, RbgA, has also revealed that the C-terminal domain is essential to the function of the protein in 50S subunit assembly but the mechanism is unclear. A mutation of the connecting loop between the GTPase domain and C-terminal RNA-binding

ANTAR domain resulted in a non-functional phenotype *in vivo* (Gulati *et al*., 2013). This mutation did not result in decreased binding and had minimal effect on 50S subunit-dependent GTPase activity, however *in vivo* it was unable to rescue the growth phenotype of RbgA-depleted cells. RbgA has been characterized to function similarly to YjeQ. The GTPase activity is maximally stimulated by the mature 50S subunit and only minimally by the immature 45S subunit. The results presented here demonstrate that the C-terminal domain of both of these circularly permutated GTPases has an additional role other than that of binding to the ribosomal particle.

4.3 Mechanism of YjeQ and RbfA interaction on the 30S Subunit

During assembly of the 30S subunit, multiple assembly factors associate with the immature subunit and catalyze formation of the decoding centre. Once the 30S subunit is mature, assembly factors must release from the subunit so that it may associate with the 50S subunit and become engaged in protein translation. It is likely that some of these assembly factors acts as chaperones to aid in folding of the decoding centre and that others act as checkpoint proteins to release from the 30S subunit upon maturation and assist in the release of other assembly factors. In the case of YjeQ, a functional interplay with RbfA has been suggested by which YjeQ causes removal of RbfA from the mature 30S subunit (Goto et al., 2011). However, the results of this study could not conclude the mechanism of RbfA removal by YjeQ and how this specific interaction could cause maturation of the 30S subunit. Based on the structure of YjeQ in complex

with the mature 30S subunit (Jomaa *et al*., 2011b), we hypothesized that the removal of RbfA could be induced by displacement of h44 upon interaction with the zinc-finger domain of YjeQ. We used the YjeQ M3 variant to evaluate the role of the zinc-finger domain in removal of RbfA.

Initial characterization of the interaction of RbfA with the 30S subunits revealed that RbfA displayed a weak binding to the mature 30S subunit (Figure 12A). In this case, the weakly bound protein was removed from the mature 30S subunit by YjeQ (Figure 12B). However, the YjeQ M3 variant was not able to remove RbfA from the mature 30S subunit but instead enhanced the binding of RbfA to the 30S subunit (Figure 13). Interestingly, both RbfA and YjeQ remained bound to the immature 30S subunit from Δ*yjeQ* cells simultaneously. This data suggests YjeQ utilizes the CTE to remove RbfA from the mature 30S subunit and when the CTE is not present, the protein binds to the 30S subunit in a conformation that is beneficial for RbfA binding.

Based on previous findings of the cryo-electron microscopy structure of RbfA in complex with the mature 30S subunit, the protein binds in the neck and causes a distortion of a portion of h44 and h45 towards the interface (Figure 5) (Datta et al., 2007). Since the binding of YjeQ to the mature 30S subunit causes a displacement of h44 in an opposing direction (Jomaa *et al*., 2011b), simultaneous binding of both of these assembly factors to the mature 30S subunit is most likely not favoured. However, on the immature 30S subunit, h44 is distorted and the flexibility of the helix might allow for both proteins to

simultaneously bind the particle (Jomaa *et al*., 2011a). Once the decoding centre is mature, RbfA would no longer be able to bind in the neck of the 30S subunit, while the zinc-finger of YjeQ is still displacing h44. The mature decoding centre would then be able to make contact with the C-terminal extension of YjeQ and signal GTP hydrolysis and release from the 30S subunit.

The results of this thesis propose a mechanism for YjeQ where by it detects maturation of the decoding centre through the zinc-finger domain. This mechanism is mediated through contact of the zinc-finger domain with the newly formed h44 following the release of RbfA from the mature 30S subunit. The model would suggest that YjeQ and RbfA are able to simultaneously bind an immature 30S subunit during late stages of ribosome biogenesis, before the decoding centre has been formed (Figure 17). The stages between binding of the assembly factors and maturation of the decoding centre remain to be elucidated, however preliminary results from our lab suggests that multiple assembly factors are able to simultaneously bind the immature 30S subunit (unpublished). These assembly factors would act as chaperones in the formation of the decoding centre and processing of the 17S rRNA to 16S rRNA. Once the 30S subunit is nearly mature, all of the assembly factors, except YjeQ, would be removed from the nearly mature 30S subunit. Following the release of all other assembly factors, h44 would interact with the zinc-finger domain of YjeQ and cause large conformational changes within the protein to signal GTP hydrolysis and removal of YjeQ. A mature 30S subunit would then be ready to enter the

translation cycle. In this proposed model YjeQ would act as a checkpoint protein. It would be present from beginning to end during maturation of the decoding centre and would only be removed once maturation is complete.

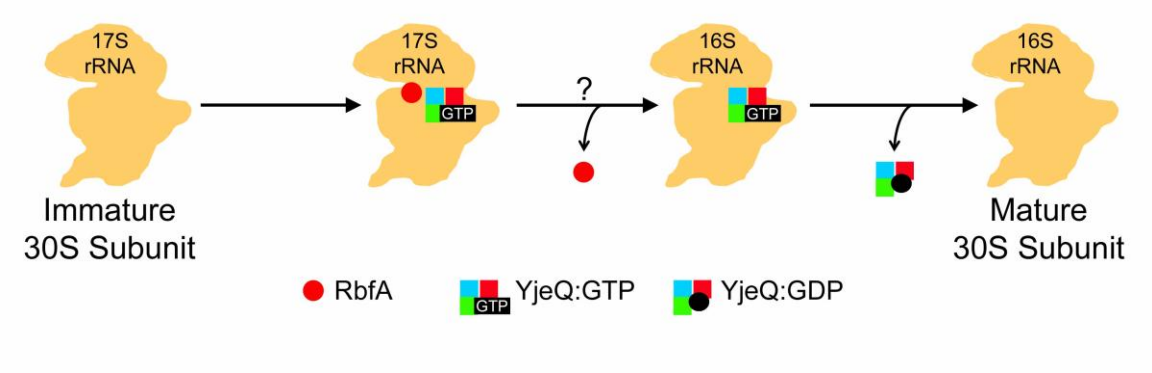

Figure 17. Model of YjeQ and RbfA interplay with the 30S particle. Schematic representing the interplay between YjeQ and RbfA during maturation of the immature 30S subunit containing 17S rRNA to the mature 30S subunit with 16S rRNA. RbfA and YjeQ simultaneously bind the immature 30S subunit. The steps of rRNA folding and processing (?) with the help of additional assembly factors remain unclear. Following maturation of the decoding centre RbfA comes off the nearly mature 30S subunit. YjeQ acts as a checkpoint protein and hydrolyzes GTP to GDP once maturation is complete so that it may be removed.

Future work aims to elucidate the cryo-electron microscopy structure of the YjeQ M3 variant bound to the 30S subunit to establish what conformational changes of h44 would be induced by the variant versus YjeQ. The cryo-EM structure of RbfA bound to the immature 30S subunit will also provide a structure of a more physiological complex of RbfA with the 30S subunit. Together these structures will provide snapshots of the assembly process and provide more depth to the mechanism of YjeQ and RbfA interplay proposed here.

5. References

Adilakshmi, T., Bellur, D.L. and Woodson, S.A. 2008. Concurrent nucleation of 16S folding and induced fit in 30S ribosome assembly. *Nature* **455**: 1268-1272.

Anand, B., Verma, S.K. and Prakash, B. 2006. Structural stabilization of GTP-binding domains in circularly permuted GTPases: implications for RNA binding. *Nucleic Acids Res.* **34**: 2196-2205.

Arigoni, F., Talabot, F., Peitsch, M., Edgerton, M.D., Meldrum, E., Allet, E., Fish, R., Jamotte, T., Curchod, M.L. and Loferer, H. 1998. A genome-based approach for the identification of essential bacterial genes. *Nat. Biotechnol.* **16**: 851-856.

Baba, T., Ara, T., Hasegawa, M., Takai, Y., Okumura, Y., Baba, M., Datsenko, K.A., Tomita, M., Wanner, B.L. and Mori, H. 2006. Construction of Escherichia coli K-12 in-frame, single-gene knockout mutants: the Keio collection. *Mol. Syst. Biol.* **2**: 2006.0008.

Boehringer, D., O'Farrell, H.C., Rife, J.P. and Ban, N. 2012. Structural insights into methyltransferase KsgA function in 30S ribosomal subunit biogenesis. *J. Biol. Chem.* **287**: 10453-10459.

Bunner, A.E., Trauger, S.A., Siuzdak, G. and Williamson, J.R. 2008. Quantitative ESI-TOF analysis of macromolecular assembly kinetics. *Anal. Chem.* **80**: 9379-9386.

Bylund, G.O., Wipemo, L.C., Lundberg, L.A. and Wikstrom, P.M. 1998. RimM and RbfA are essential for efficient processing of 16S rRNA in Escherichia coli. *J. Bacteriol.* **180**: 73-82.

Campbell, T.L. and Brown, E.D. 2008. Genetic interaction screens with ordered overexpression and deletion clone sets implicate the Escherichia coli GTPase YjeQ in late ribosome biogenesis. *J. Bacteriol.* **190**: 2537-2545.

Chen, S.S. and Williamson, J.R. 2013. Characterization of the Ribosome Biogenesis Landscape in E. coli Using Quantitative Mass Spectrometry. *J. Mol. Biol.* **425**: 767-779.

Clatterbuck Soper, S.F., Dator, R.P., Limbach, P.A. and Woodson, S.A. 2013. In vivo X-ray footprinting of pre-30S ribosomes reveals chaperone-dependent remodeling of late assembly intermediates. *Mol. Cell* **52**: 506-516.

Connolly, K. and Culver, G. 2013. Overexpression of RbfA in the absence of the KsgA checkpoint results in impaired translation initiation. *Mol. Microbiol.*

Daigle, D.M. and Brown, E.D. 2004. Studies of the interaction of Escherichia coli YjeQ with the ribosome in vitro. *J. Bacteriol.* **186**: 1381-1387.

Daigle, D.M., Rossi, L., Berghuis, A.M., Aravind, L., Koonin, E.V. and Brown, E.D. 2002. YjeQ, an essential, conserved, uncharacterized protein from Escherichia coli, is an unusual GTPase with circularly permuted G-motifs and marked burst kinetics. *Biochemistry* **41**: 11109-11117.

Dammel, C.S. and Noller, H.F. 1995. Suppression of a cold-sensitive mutation in 16S rRNA by overexpression of a novel ribosome-binding factor, RbfA. *Genes Dev.* **9**: 626-637.

Datta, P.P., Wilson, D.N., Kawazoe, M., Swami, N.K., Kaminishi, T., Sharma, M.R., Booth, T.M., Takemoto, C., Fucini, P., Yokoyama, S. et al. 2007. Structural aspects of RbfA action during small ribosomal subunit assembly. *Mol. Cell* **28**: 434-445.

Davies, B.W., Kohrer, C., Jacob, A.I., Simmons, L.A., Zhu, J., Aleman, L.M., Rajbhandary, U.L. and Walker, G.C. 2010. Role of Escherichia coli YbeY, a highly conserved protein, in rRNA processing. *Mol. Microbiol.* **78**: 506-518.

de Narvaez, C.C. and Schaup, H.W. 1979. In vivo transcriptionally coupled assembly of Escherichia coli ribosomal subunits. *J. Mol. Biol.* **134**: 1-22.

Elias, M. and Novotny, M. 2008. cpRAS: a novel circularly permuted RAS-like GTPase domain with a highly scattered phylogenetic distribution. *Biol. Direct* **3**: 21-6150-3-21.

Ginsburg, D. and Steitz, J.A. 1975. The 30 S ribosomal precursor RNA from Escherichia coli. A primary transcript containing 23 S, 16 S, and 5 S sequences. *J. Biol. Chem.* **250**: 5647-5654.

Goto, S., Kato, S., Kimura, T., Muto, A. and Himeno, H. 2011. RsgA releases RbfA from 30S ribosome during a late stage of ribosome biosynthesis. *Embo j.* **30**: 104-114.

Greenfield, N. and Fasman, G.D. 1969. Computed circular dichroism spectra for the evaluation of protein conformation. *Biochemistry* **8**: 4108-4116.

Greenfield, N.J. 2006. Using circular dichroism spectra to estimate protein secondary structure. *Nat. Protoc.* **1**: 2876-2890.

Gulati, M., Jain, N., Anand, B., Prakash, B. and Britton, R.A. 2013. Mutational analysis of the ribosome assembly GTPase RbgA provides insight into ribosome interaction and ribosome-stimulated GTPase activation. *Nucleic Acids Res.* **41**: 3217-3227.

Guo, Q., Goto, S., Chen, Y., Feng, B., Xu, Y., Muto, A., Himeno, H., Deng, H., Lei, J. and Gao, N. 2013. Dissecting the in vivo assembly of the 30S ribosomal subunit reveals the role of RimM and general features of the assembly process. *Nucleic Acids Res.* **41**: 2609-2620.

Guo, Q., Yuan, Y., Xu, Y., Feng, B., Liu, L., Chen, K., Sun, M., Yang, Z., Lei, J. and Gao, N. 2011. Structural basis for the function of a small GTPase RsgA on the 30S ribosomal subunit maturation revealed by cryoelectron microscopy. *Proc. Natl. Acad. Sci. U. S. A.* **108**: 13100-13105.

Hase, Y., Yokoyama, S., Muto, A. and Himeno, H. 2009. Removal of a ribosome small subunit-dependent GTPase confers salt resistance on Escherichia coli cells. *Rna* **15**: 1766-1774.

Held, W.A., Ballou, B., Mizushima, S. and Nomura, M. 1974. Assembly mapping of 30 S ribosomal proteins from Escherichia coli. Further studies. *J. Biol. Chem.* **249**: 3103-3111.

Himeno, H., Hanawa-Suetsugu, K., Kimura, T., Takagi, K., Sugiyama, W., Shirata, S., Mikami, T., Odagiri, F., Osanai, Y., Watanabe, D. et al. 2004. A novel GTPase activated by the small subunit of ribosome. *Nucleic Acids Res.* **32**: 5303-5309.

Holzwarth, G. and Doty, P. 1965. The Ultraviolet Circular Dichroism of Polypeptides. *J. Am. Chem. Soc.* **87**: 218-228.

Inoue, K., Alsina, J., Chen, J. and Inouye, M. 2003. Suppression of defective ribosome assembly in a rbfA deletion mutant by overexpression of Era, an essential GTPase in Escherichia coli. *Mol. Microbiol.* **48**: 1005-1016.

Inoue, K., Chen, J., Tan, Q. and Inouye, M. 2006. Era and RbfA have overlapping function in ribosome biogenesis in Escherichia coli. *J. Mol. Microbiol. Biotechnol.* **11**: 41-52.

Jacob, A.I., Kohrer, C., Davies, B.W., RajBhandary, U.L. and Walker, G.C. 2013. Conserved bacterial RNase YbeY plays key roles in 70S ribosome quality control and 16S rRNA maturation. *Mol. Cell* **49**: 427-438.

Jomaa, A., Jain, N., Davis, J.H., Williamson, J.R., Britton, R.A. and Ortega, J. 2014. Functional domains of the 50S subunit mature late in the assembly process. *Nucleic Acids Res.* **42**: 3419-3435.

Jomaa, A., Stewart, G., Martin-Benito, J., Zielke, R., Campbell, T.L., Maddock, J.R., Brown, E.D. and Ortega, J. 2011a. Understanding ribosome assembly: the structure of in vivo assembled immature 30S subunits revealed by cryo-electron microscopy. *Rna* **17**: 697-709.

Jomaa, A., Stewart, G., Mears, J.A., Kireeva, I., Brown, E.D. and Ortega, J. 2011b. Cryo-electron microscopy structure of the 30S subunit in complex with the YjeQ biogenesis factor. *Rna* **17**: 2026-2038.

Jones, P.G. and Inouye, M. 1996. RbfA, a 30S ribosomal binding factor, is a cold-shock protein whose absence triggers the cold-shock response. *Mol. Microbiol.* **21**: 1207-1218.

Kaltschmidt, E. and Wittmann, H.G. 1970. Ribosomal proteins. XII. Number of proteins in small and large ribosomal subunits of Escherichia coli as determined by two-dimensional gel electrophoresis. *Proc. Natl. Acad. Sci. U. S. A.* **67**: 1276-1282.

Kim do, J., Jang, J.Y., Yoon, H.J. and Suh, S.W. 2008. Crystal structure of YlqF, a circularly permuted GTPase: implications for its GTPase activation in 50 S ribosomal subunit assembly. *Proteins* **72**: 1363-1370.

Kimura, T., Takagi, K., Hirata, Y., Hase, Y., Muto, A. and Himeno, H. 2008. Ribosome-small-subunit-dependent GTPase interacts with tRNA-binding sites on the ribosome. *J. Mol. Biol.* **381**: 467-477.

Kitagawa, M., Ara, T., Arifuzzaman, M., Ioka-Nakamichi, T., Inamoto, E., Toyonaga, H. and Mori, H. 2005. Complete set of ORF clones of Escherichia coli ASKA library (a complete set of E. coli K-12 ORF archive): unique resources for biological research. *DNA Res.* **12**: 291-299.

Krishna, S.S., Majumdar, I. and Grishin, N.V. 2003. Structural classification of zinc fingers: survey and summary. *Nucleic Acids Res.* **31**: 532-550.

Leipe, D.D., Wolf, Y.I., Koonin, E.V. and Aravind, L. 2002. Classification and evolution of P-loop GTPases and related ATPases. *J. Mol. Biol.* **317**: 41-72.

Leong, V., Kent, M., Jomaa, A. and Ortega, J. 2013. Escherichia coli rimM and yjeQ null strains accumulate immature 30S subunits of similar structure and protein complement. *Rna* **19**: 789-802.

Lescoute, A. and Westhof, E. 2006. The A-minor motifs in the decoding recognition process. *Biochimie* **88**: 993-999.

Levdikov, V.M., Blagova, E.V., Brannigan, J.A., Cladiere, L., Antson, A.A., Isupov, M.N., Seror, S.J. and Wilkinson, A.J. 2004. The crystal structure of YloQ, a circularly permuted GTPase essential for Bacillus subtilis viability. *J. Mol. Biol.* **340**: 767-782.

Li, N., Chen, Y., Guo, Q., Zhang, Y., Yuan, Y., Ma, C., Deng, H., Lei, J. and Gao, N. 2013. Cryo-EM structures of the late-stage assembly intermediates of the bacterial 50S ribosomal subunit. *Nucleic Acids Res.* **41**: 7073-7083.

Li, Z., Pandit, S. and Deutscher, M.P. 1999. RNase G (CafA protein) and RNase E are both required for the 5' maturation of 16S ribosomal RNA. *Embo j.* **18**: 2878-2885.

Lindahl, L. 1975. Intermediates and time kinetics of the in vivo assembly of Escherichia coli ribosomes. *J. Mol. Biol.* **92**: 15-37.

Mizushima, S. and Nomura, M. 1970. Assembly mapping of 30S ribosomal proteins from E. coli. *Nature* **226**: 1214.

Mulder, A.M., Yoshioka, C., Beck, A.H., Bunner, A.E., Milligan, R.A., Potter, C.S., Carragher, B. and Williamson, J.R. 2010. Visualizing ribosome biogenesis: parallel assembly pathways for the 30S subunit. *Science* **330**: 673-677.

Nichols, C.E., Johnson, C., Lamb, H.K., Lockyer, M., Charles, I.G., Hawkins, A.R. and Stammers, D.K. 2007. Structure of the ribosomal interacting GTPase YjeQ from the enterobacterial species Salmonella typhimurium. *Acta Crystallogr. Sect. F. Struct. Biol. Cryst. Commun.* **63**: 922-928.

Nierhaus, K.H. and Dohme, F. 1974. Total reconstitution of functionally active 50S ribosomal subunits from Escherichia coli. *Proc. Natl. Acad. Sci. U. S. A.* **71**: 4713-4717.

Rohl, R. and Nierhaus, K.H. 1982. Assembly map of the large subunit (50S) of Escherichia coli ribosomes. *Proc. Natl. Acad. Sci. U. S. A.* **79**: 729-733.

Sabate, R., de Groot, N.S. and Ventura, S. 2010. Protein folding and aggregation in bacteria. *Cell Mol. Life Sci.* **67**: 2695-2715.

Sambrook, J., Fritsch, E. and Maniatis, T. 1989. *Molecular cloning: a laboratory manual.* Cold Spring Harbor Laboratory Press, Cold Spring Harbor, NY.

Sayed, A., Matsuyama, S. and Inouye, M. 1999. Era, an essential Escherichia coli small G-protein, binds to the 30S ribosomal subunit. *Biochem. Biophys. Res. Commun.* **264**: 51-54.

Shajani, Z., Sykes, M.T. and Williamson, J.R. 2011. Assembly of bacterial ribosomes. *Annu. Rev. Biochem.* **80**: 501-526.

Sharma, M.R., Barat, C., Wilson, D.N., Booth, T.M., Kawazoe, M., Hori-Takemoto, C., Shirouzu, M., Yokoyama, S., Fucini, P. and Agrawal, R.K. 2005. Interaction of Era with the 30S ribosomal subunit implications for 30S subunit assembly. *Mol. Cell* **18**: 319-329.

Shin, D.H., Lou, Y., Jancarik, J., Yokota, H., Kim, R. and Kim, S.H. 2004. Crystal structure of YjeQ from Thermotoga maritima contains a circularly permuted GTPase domain. *Proc. Natl. Acad. Sci. U. S. A.* **101**: 13198-13203.

Spillmann, S., Dohme, F. and Nierhaus, K.H. 1977. Assembly in vitro of the 50 S subunit from Escherichia coli ribosomes: proteins essential for the first heat-dependent conformational change. *J. Mol. Biol.* **115**: 513-523.

Sprang, S.R. 1997. G protein mechanisms: insights from structural analysis. *Annu. Rev. Biochem.* **66**: 639-678.

Strunk, B.S. and Karbstein, K. 2009. Powering through ribosome assembly. *Rna* **15**: 2083-2104.

Sudhamsu, J., Lee, G.I., Klessig, D.F. and Crane, B.R. 2008. The structure of YqeH. An AtNOS1/AtNOA1 ortholog that couples GTP hydrolysis to molecular recognition. *J. Biol. Chem.* **283**: 32968-32976.

Sulthana, S. and Deutscher, M.P. 2013. Multiple exoribonucleases catalyze maturation of the 3' terminus of 16S ribosomal RNA (rRNA). *J. Biol. Chem.* **288**: 12574-12579.

Talkington, M.W., Siuzdak, G. and Williamson, J.R. 2005. An assembly landscape for the 30S ribosomal subunit. *Nature* **438**: 628-632.

Theobald, D.L., Mitton-Fry, R.M. and Wuttke, D.S. 2003. Nucleic acid recognition by OB-fold proteins. *Annu. Rev. Biophys. Biomol. Struct.* **32**: 115-133.

Tissieres, A. and Watson, J.D. 1958. Ribonucleoprotein particles from Escherichia coli. *Nature* **182**: 778-780.

Traub, P. and Nomura, M. 1968. Structure and function of E. coli ribosomes. V. Reconstitution of functionally active 30S ribosomal particles from RNA and proteins. *Proc. Natl. Acad. Sci. U. S. A.* **59**: 777-784.

Wachi, M., Umitsuki, G., Shimizu, M., Takada, A. and Nagai, K. 1999. Escherichia coli cafA gene encodes a novel RNase, designated as RNase G, involved in processing of the 5' end of 16S rRNA. *Biochem. Biophys. Res. Commun.* **259**: 483-488.

Wilson, D.N. and Nierhaus, K.H. 2007. The weird and wonderful world of bacterial ribosome regulation. *Crit. Rev. Biochem. Mol. Biol.* **42**: 187-219.

Wimberly, B.T., Brodersen, D.E., Clemons, W.M.,Jr, Morgan-Warren, R.J., Carter, A.P., Vonrhein, C., Hartsch, T. and Ramakrishnan, V. 2000. Structure of the 30S ribosomal subunit. *Nature* **407**: 327-339.

Xia, B., Ke, H., Shinde, U. and Inouye, M. 2003. The role of RbfA in 16S rRNA processing and cell growth at low temperature in Escherichia coli. *J. Mol. Biol.* **332**: 575-584.

Yang, Z., Guo, Q., Goto, S., Chen, Y., Li, N., Yan, K., Zhang, Y., Muto, A., Deng, H., Himeno, H. et al. 2014. Structural insights into the assembly of the 30S ribosomal subunit in vivo: functional role of S5 and location of the 17S rRNA precursor sequence. *Protein Cell.*